

Analysis and Simulations for a Phase Field Fracture Model at Finite Strains

M. Thomas ^{*} C. Bilgen [†] K. Weinberg [‡]

April 19, 2017

Abstract

Phase-field models have already been proven to predict complex fracture patterns in two and three dimensions for brittle fracture. In this paper we discuss a model for phase-field fracture at finite deformations in more detail. Among the identification of crack location and projection of crack growth the numerical stability is one of the main challenges in solid mechanics. In a first step to investigate these assignments precisely we introduce a suitable weak formulation of the model and propose a numerical solution method in terms of time and space discretization. Second the mathematical background of the approach is examined and we show that the time-discrete solutions converge in a weak sense to a solution of the time-continuous formulation. The analytically proven approximation property is verified within numerical examples in two and three dimensions.

1 Introduction

In solid mechanics one of the main challenges is the prediction of crack growth and fragmentation patterns. Regarding to the modeling side complicated structures and non-regular behavior of cracks turn numerical simulations into a difficult task. The classical brittle fracture approach of Griffith and Irwin [Gri21, Irw58] is based on an energy minimization setting for the whole structure. Let us consider a solid with domain $\mathcal{B}_0 \subset \mathbb{R}^3$ and boundary $\partial\mathcal{B}_0 \equiv \Gamma \subset \mathbb{R}^2$ deforming within a time interval $t \in [0, T] \subset \mathbb{R}^+$. Each crack that is located in a solid forms a new boundary surface $\Gamma(t)$ of a priori unknown position which needs to be identified. Therefore, the total potential energy of a homogenous but cracking solid is composed of its material's energy with a free Helmholtz energy density Ψ and of surface energy contributions from growing crack boundaries.

$$E = \int_{\mathcal{B}_0} \Psi \, dX + \int_{\Gamma(t)} \mathcal{G}_c \, d\Gamma. \quad (1.1)$$

For brittle fracture the material's resistance to cracking \mathcal{G}_c corresponds to the Griffith's critical energy release rate. However, the optimization of the energy functional (1.1) is a challenging task and can not be deduced in general because of the moving boundary $\Gamma(t)$. Several sophisticated discretization techniques exist, e.g. cohesive zone models [Xu94, Or99, Roe03], eroded finite elements [Mar03, Suk03] or eigenfracture strategies [Schm09, Pan12] to name some of them. In order to compute such moving boundary problems, the focus is set on a phase-field model that is a diffuse-interface approach and has gained attention to similar problems recently formulated in literature [HL04, Kar01, Mie10PF, Bor13, Bor12]. The main idea of this ansatz is to mark the material's state of the body by a continuous order parameter $s(\mathbf{x}, t)$ which evolves in space \mathbf{x} and time t .

^{*}Weierstrass Institute for Applied Analysis and Stochastics, Mohrenstr. 39, 10117 Berlin, Germany. Email: marita.thomas@wias-berlin.de

[†]Lehrstuhl für Festkörpermechanik, Department Maschinenbau, Universität Siegen, Paul-Bonatz-Straße 9-11, 57068 Siegen, Germany. Email: carola.bilgen@uni-siegen.de

[‡]Lehrstuhl für Festkörpermechanik, Department Maschinenbau, Universität Siegen, Paul-Bonatz-Straße 9-11, 57068 Siegen, Germany. Email: kerstin.weinberg@uni-siegen.de

Because many different applications in solid mechanics can become very complex, it is important to ensure the stability of the numerical simulation and the existence of a solution. Therefore, the mathematical mathematical properties of the model and its numerical approximation strategy have to be investigated in detail.

In the remaining part of the paper we will proceed as follows: In the next section we present the basic equations of the phase-field approach to fracture for finite deformations and the spatial and temporal discretization is provided. In Sect. 3 the analytical setup is introduced and, based on this, the time-discretization proposed in Sect. 2 is revisited. In particular, it is proven that solutions constructed with the time-discrete scheme converge to a solution of the time-continuous weak formulation. This convergence result is confirmed within a series of numerical examples in Sect. 4. We demonstrate one two dimensional example for a simple but typical problem of a mode-I-tension test to study different influencing factors. Further, three dimensional examples are presented, amongst others a phase-field Benchmark problem proposed in the framework of our DFG Priority Programm 1748, cf. [Mue2016]. Our numerical results match with the proven analytical results.

2 Basic Equations

In the following the phase-field model and the related equations are proposed and examined in more detail. The phase-field is by definition a continuous field and thus, the moving crack boundaries are 'smeared' over a small but finite length. The order parameter $s(\mathbf{x}, t) : \mathcal{B}_0 \times [0, T] \rightarrow \mathbb{R}$ with $s \in [0, 1]$ characterizes the state of material, whereby $s = 1$ indicates the unbroken state and $s = 0$ the broken state. The surface integral in (1.1) is approximated by a regularization using a crack density function $\gamma : \mathbb{R} \times \mathbb{R}^3 \rightarrow [0, \infty)$:

$$\int_{\Gamma(t)} d\Gamma \approx \int_{\mathcal{B}_0} \gamma(s(\mathbf{x}, t), \nabla s(\mathbf{x}, t)) dX \quad (2.1)$$

This approximation (2.1) is inserted in the total potential energy (1.1) so that the optimization problem can be formulated locally:

$$E = \int_{\mathcal{B}_0} (\Psi + \mathcal{G}_c \gamma) d\mathcal{B}_0 \rightarrow \text{optimum} \quad (2.2)$$

There exist different ways to choose the crack density function which is only different from zero along cracks by definition. Typically a second-order phase-field approach is defined as:

$$\gamma(s, \nabla s) := \frac{1}{2l_c} (1 - s)^2 + \frac{l_c}{2} |\nabla s|^2 \quad (2.3)$$

with the fixed parameter $l_c \in (0, 1)$ which is a measure for the width of the diffuse interface zone, see Fig. 5. Furthermore, the length-scale parameter l_c weights the influence of the linear and the gradient

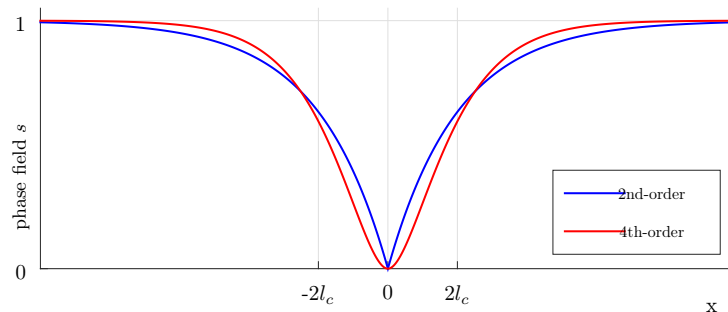


Figure 1: Uniaxial model with a crack at $x = 0$ and with a continuous phase field $s \in [0, 1]$; phase field approximation for a second order and a fourth order approximation of crack density function γ .

term whereby the gradient enforces the regularization of the sharp interface. The insertion of (2.3) in (2.2) leads to a potential which is related to the work of Ambrosio and Tortorelli [AT1990]. The evolution equation of the phase-field is stated in a general form

$$\dot{s} = MY, \quad (2.4)$$

where the parameter M denotes the kinematic mobility and Y summarizes all driving forces which typically represent a competition of bulk material and surface forces.

$$Y = \delta_s(\Psi + \mathcal{G}_c\gamma) = \delta_s\Psi + \mathcal{G}_c\delta_s\gamma \quad (2.5)$$

In particular, the phase-field model is based on the crack density function (2.3) and the driving force for crack growth that consists of components of the free energy. The governing balance equations for the phase-field fracture are summarized in Table 1 whereas we will focus on quasi-static simulations in this paper such that the inertia terms in the balance of linear momentum will be neglected.

Table 1: Balance equations for a cracking solid subjected to body forces $\bar{\mathbf{b}}$ in \mathcal{B}_0 , prescribed deformations $\bar{\varphi}$ on $\partial\mathcal{B}_0^D$ and tractions $\bar{\mathbf{t}}$ on $\partial\mathcal{B}_0^N$ with $\partial\mathcal{B}_0^D \cup \partial\mathcal{B}_0^N = \partial\mathcal{B}_0$.

Balance of linear momentum:	$\operatorname{div}(\mathbf{P}) + \bar{\mathbf{b}} = \rho_0\dot{\varphi}$	on \mathcal{B}_0
Boundary conditions:	$\varphi = \bar{\varphi}$	on $\partial\mathcal{B}_0^D$
	$\mathbf{P} \cdot \bar{\mathbf{n}} = \bar{\mathbf{t}}$	on $\partial\mathcal{B}_0^N$
Phase-field equation:	$M \left(\frac{\partial\Psi}{\partial s} - \frac{\mathcal{G}_c}{l_c}(1-s) - \mathcal{G}_cl_c\Delta s \right) = \dot{s}$	on \mathcal{B}_0
Boundary conditions:	$s = 1$	on $\partial\mathcal{B}_0^D$
	$\nabla s \cdot \bar{\mathbf{n}} = 0$	on $\partial\mathcal{B}_0^N$

Because we set the focus on finite strains, a nonlinear material model and their split into compressive and tensile parts which are only responsible for crack growth are considered in the following.

2.1 Finite elasticity

In the finite deformation regime a deformation mapping $\varphi(\mathbf{X}, t) : \mathcal{B}_0 \times [0, T] \rightarrow \mathbb{R}^3$ is considered and the deformation gradient $\mathbf{F} : \mathcal{B}_0 \times [0, T] \rightarrow \mathbb{R}^{3 \times 3}$ is defined as

$$\mathbf{F} = \nabla_{\mathbf{X}}\varphi = \frac{\partial\varphi}{\partial\mathbf{X}}. \quad (2.6)$$

Regarding the following notation the fields in capitals refer to the initial configuration. Furthermore, the area vectors are mapped from the reference to the current configuration by using the so called cofactor $\mathbf{H} : \mathcal{B}_0 \times [0, T] \rightarrow \mathbb{R}^{3 \times 3}$ which is based on the definition of the tensor cross product introduced in [Bon15]

$$\mathbf{H} = \operatorname{cof}(\mathbf{F}) = \frac{1}{2}(\mathbf{F} \times \mathbf{F}). \quad (2.7)$$

The volume map $J : \mathcal{B}_0 \times [0, T] \rightarrow \mathbb{R}$ is also presented with the tensor cross product and is given by

$$J = \det(\mathbf{F}) = \frac{1}{6}(\mathbf{F} \times \mathbf{F}) : \mathbf{F}. \quad (2.8)$$

By making use of the proposed extended kinematic set the free energy Ψ can be rewritten such that the strain energy function fulfils the characteristic of polyconvexity, see Definition 3.1, which ensures the existence of a minimum and a stable numerical approximation. We will refer to the mathematical point of view in more detail in Sect. 3.1. Hence, the strain energy function becomes

$$\Psi = W(\mathbf{F}, \mathbf{H}, J). \quad (2.9)$$

Moreover, the first Piola-Kirchhoff stress tensor \mathbf{P} can be formulated as

$$\mathbf{P} = \frac{\partial W}{\partial \mathbf{F}} + \frac{\partial W}{\partial \mathbf{H}} \times \mathbf{F} + \frac{\partial W}{\partial J} \mathbf{H}. \quad (2.10)$$

To take into account the anisotropy of fracture, in particular that only the tensile parts of the strain energy function contribute the crack growth an anisotropic split has to be deduced. For that reason the strain energy function (2.9) is formulated by using the invariants $I_C = J^{-2/3} \mathbf{F} : \mathbf{F}$ and $II_C = J^{-4/3} \mathbf{H} : \mathbf{H}$ which are based on the isochoric split of the deformation gradient $\bar{\mathbf{F}} = J^{-1/3} \mathbf{F}$. This split decomposes the deformation in a volumetric and an isochoric part to regard different behavior of the material in bulk and shear. Then the invariants are decomposed in compressive and tensile parts as proposed in [Hesch17]

$$I_C^\pm = 3 + J^{-2/3} \langle \mathbf{F} : \mathbf{F} - 3 \rangle^\pm, \quad (2.11)$$

$$II_C^\pm = 3 + J^{-4/3} \langle \mathbf{H} : \mathbf{H} - 3 \rangle^\pm, \quad (2.12)$$

$$J^\pm = 1 + \langle J - 1 \rangle^\pm. \quad (2.13)$$

This anisotropic split is presented in Fig. 2 by way of example for the first invariant visually.

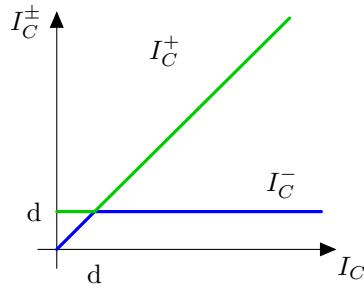


Figure 2: Illustration of the anisotropic split of the first invariant into tensile and compressive parts with dimension $d \in \{2, 3\}$.

In consequence, the energy W is also split into tension induced and compression induced components

$$W(\mathbf{F}, \mathbf{H}, J, s) = \beta(s)W(I_C^+, II_C^+, J^+) + W(I_C^-, II_C^-, J^-) \quad (2.14)$$

whereas the degradation function β is given by

$$\beta : [0, 1] \rightarrow [\eta, \infty), \quad \beta(s) := (\eta + s^2). \quad (2.15)$$

The parameter η is a very small value $\eta \ll 1$ to catch numerical instabilities in the limit cases for the phase-field.

2.2 Discretization

In this subsection the weak forms and the discretization are considered in more detail. The elastic boundary value problem is based on the balance of linear momentum and the crack phase-field evolution, cf. Table 1. For fixed time, these equations are rewritten in the weak form and the coupled problem reads: Find $\varphi \in \mathcal{B}_0$ and $s \in [0, 1]$ such that

$$\int_{\mathcal{B}_0} \mathbf{P} : \nabla(\delta\varphi) \, d\mathcal{B}_0 = \int_{\mathcal{B}_0} \bar{\mathbf{b}} \cdot \delta\varphi \, d\mathcal{B}_0 + \int_{\partial\mathcal{B}_0^N} \bar{\mathbf{t}} \cdot \delta\varphi \, d\Gamma \quad \forall \delta\varphi \in \mathbf{U}, \quad (2.16)$$

and

$$\int_{\mathcal{B}_0} \dot{s} \cdot \delta s \, d\mathcal{B}_0 + \int_{\mathcal{B}_0} \frac{\partial \Psi}{\partial s} \cdot \delta s \, d\mathcal{B}_0 + 2\mathcal{G}_c l_c \int_{\mathcal{B}_0} \nabla s \nabla(\delta s) \, d\mathcal{B}_0 - \frac{\mathcal{G}_c}{2l_c} \int_{\mathcal{B}_0} (1-s) \cdot \delta s \, d\mathcal{B}_0 = 0 \quad \forall \delta s \in \mathbf{X}. \quad (2.17)$$

The fraction $\frac{\partial \Psi}{\partial s}$ in (2.17) serves as a driving force for the phase-field. Moreover, the spaces of admissible test functions \mathbf{U} and \mathbf{X} are defined as $\mathbf{U} = \{\varphi \in H^1(\mathcal{B}_0; \mathbb{R}^3) \mid \delta \varphi = 0 \text{ on } \partial \mathcal{B}_0\}$, where $H^1(\mathcal{B}_0; \mathbb{R}^3)$ denotes the Sobolev functional space of square integrable functions with values in \mathbb{R}^3 and with square integrable weak first derivatives. Correspondingly the space of admissible test functions for the phase-field equation can be formulated as $\mathbf{X} = \{\delta s \in H^1(\mathcal{B}_0) \cap L^\infty(\mathcal{B}_0) \mid \delta s = 1 \text{ on } \partial \mathcal{B}_0\}$.

To apply the finite element method in the following the domain \mathcal{B}_0 is subdivided into a finite set of non-overlapping elements

$$\mathcal{B}_0 \approx \mathcal{B}_0^h = \bigcup_{e=1}^{n_e} \mathcal{B}_{0e}. \quad (2.18)$$

Furthermore, within the discretization we use Lagrangian polynomials for both fields. In particular, the ansatzfunctions for the mechanical field are denoted by N_i and the shape functions for the phase-field by \tilde{N}_i . The values $\hat{\varphi}^{(i)}$ and $\hat{s}^{(i)}$ are the nodal displacements and the nodal values for the phase-field.

$$\varphi \approx \varphi^h = \sum_{i=1}^{n_k} N_i \hat{\varphi}^{(i)}, \quad \delta \varphi^h = \sum_{i=1}^{n_k} N_i \delta \hat{\varphi}^{(i)}, \quad (2.19)$$

$$s \approx s^h = \sum_{i=1}^{n_k} \tilde{N}_i \hat{s}^{(i)}, \quad \delta s^h = \sum_{i=1}^{n_k} \tilde{N}_i \delta \hat{s}^{(i)}. \quad (2.20)$$

Inserting the proposed approximations (2.19) and (2.20) into the weak formulations (2.16) and (2.17) the final finite element system results after a straightforward calculation. The time integration is based on an implicit Euler-backward scheme regarding the phase-field parameter s , whereby the time interval $[0, T]$ is divided into pairwise disjoint equidistant subintervals with the time step $\Delta t := t_{n+1} - t_n$. At last the system of equations is solved by making use of the Gaussian elimination method. There exist two popular solution strategies for the non-linear system (2.16) and (2.17), the monolithic and the staggered scheme. Making use of the first mentioned ansatz the fully-coupled system is solved in each timestep; using the staggered scheme the solving part is split into the phase-field s and the mechanical field φ which means that in each timestep both quantities are solved successively. For the analysis in Sect. 3 we will use this latter approach. Further information about different solution strategies can be found in [Bil17].

3 Analytical Setup, Discretization, and Convergence Result

For the mathematical analysis of the regularized crack model given by equations (2.16)–(2.17) we define the free energy functional $\mathcal{E} : [0, T] \times \mathbf{U} \times \mathbf{Z} \rightarrow \mathbb{R}$,

$$\mathcal{E}(t, \varphi, s) := \int_{\mathcal{B}_0} (\beta(s)W_1(\mathbb{M}\nabla\varphi) + W_2(\mathbb{M}\nabla\varphi) + \gamma(s, \nabla s)) \, dX + \int_{\partial \mathcal{B}_0^N} \mathbf{h} \cdot \varphi \, d\mathcal{H}^2 \quad (3.1)$$

on suitable Banach spaces \mathbf{U}, \mathbf{Z} with $\gamma : \mathbb{R} \times \mathbb{R}^3 \rightarrow [0, \infty)$ from (2.3) and $\beta : \mathbb{R} \rightarrow [\eta, \infty)$, with $\beta(s) := \eta + s^2$ as in (2.15). Moreover,

$$\mathbb{M} : \mathbb{R}^{3 \times 3} \rightarrow \mathbb{R}^{3 \times 3} \times \mathbb{R}^{3 \times 3} \times \mathbb{R}, \quad \mathbb{M}F := (F, \text{cof } F, \det F) \quad (3.2)$$

maps a 3×3 -matrix onto the vector of its minors and the properties of the densities $W_i : \mathbb{R}^{3 \times 3} \times \mathbb{R}^{3 \times 3} \times \mathbb{R} \rightarrow \mathbb{R}$ are specified more precisely in Sec. 3.1.

In addition, we introduce the viscous dissipation potential $\mathcal{V}_\alpha : \mathbf{Z} \rightarrow [0, \infty)$

$$\mathcal{V}_\alpha(\dot{s}) := \int_{\mathcal{B}_0} \left(\frac{M^{-1}}{2} |\dot{s}|^2 + \alpha I_{(-\infty, 0]}(\dot{s}) \right) \, dX \quad (3.3)$$

with M^{-1} the inverse of the kinematic mobility M and $I_{(-\infty,0]} : \mathbb{R} \rightarrow \{0, \infty\}$ the characteristic function of the nonnegative real line, i.e., $I_{(-\infty,0]}(z) = 0$ if $z \in (-\infty, 0]$ and $I_{(-\infty,0]}(z) = \infty$ otherwise. This constraint forces the time derivative \dot{s} to take its values $(-\infty, 0]$. According to the definition $s = 1$ for the unbroken and $s = 0$ for the completely broken state of the material, it thus ensures that the damage of the material can only increase in time, i.e. the unidirectionality of the damage evolution. With the prefactor $\alpha = \text{const}$ we indicate that we switch this constraint on or off, so that we can consider two different types of models: A model with $\alpha = \text{const} > 0$, where the unidirectionality constraint is active, and a model where $\alpha = 0$, where unidirectionality is not incorporated (i.e. $0 \cdot \infty = 0$).

The elastic body undergoing damage is thus characterized by a suitable state space $\mathbf{U} \times \mathbf{Z}$, the energy functional \mathcal{E} from (3.1) and the dissipation potential \mathcal{V}_α from (3.3) and we refer to it as the (evolution) system $(\mathbf{U} \times \mathbf{Z}, \mathcal{E}, \mathcal{V}_\alpha)$

In accordance with Section 2 we will show in Thm. 3.10 that a solution $(\varphi, s) : [0, T] \rightarrow \mathbf{U} \times \mathbf{Z}$ of system $(\mathbf{U} \times \mathbf{Z}, \mathcal{E}, \mathcal{V}_\alpha)$ is characterized for a.a. $t \in (0, T)$ by

$$\text{for all } \tilde{\varphi} \in \mathbf{U} : \mathcal{E}(t, \varphi(t), s(t)) \leq \mathcal{E}(t, \tilde{\varphi}, s(t)), \quad (3.4a)$$

$$\text{if } \alpha = 0 : M^{-1}\dot{s}(t) + \beta'(s(t))W_1(\mathbb{M}\nabla\varphi(t)) + \omega'(s(t)) - \Delta s(t) = 0 \text{ in } \mathbf{X}^*, \quad (3.4b)$$

$$\text{if } \alpha > 0 : M^{-1}\dot{s}(t) + \beta'(s(t))W_1(\mathbb{M}\nabla\varphi(t)) + \omega'(s(t)) - \Delta s(t) \geq 0 \text{ in } (\mathbf{X}_-)^*, \quad (3.4c)$$

with \mathbf{X}^* the dual of the Banach space \mathbf{X} and $(\mathbf{X}_-)^*$ the elements of \mathbf{X}^* restricted to elements of $\mathbf{X}_- := \{v \in \mathbf{X}, v \leq 0\}$. While, under the assumptions of [Bal02, Thm. 2.4], minimality condition (3.4a) is equivalent to (the weak formulation in \mathbf{U} of) its Euler-Lagrange equation, which is the weak formulation of the mechanical force balance (2.16), the interpretation of (3.4b) & (3.4c) is more involved: On the one hand, observe that minimizers in the damage variable s for the energy functional can be obtained for $\mathbf{Z} := H^1(\mathcal{B}_0)$ and a minimizer will in fact satisfy $s \in \mathbf{X} := H^1(\mathcal{B}_0) \cap L^\infty(\mathcal{B}_0)$. On the other hand, due to the quadratic growth of \mathcal{V}_α it would be a first choice to understand (3.4b), resp. (3.4c), as an L^2 -gradient flow. However, $\beta'(s(t))W_1(\mathbb{M}\nabla\varphi(t)) + \omega'(s(t)) - \Delta s(t) \in L^2(\Omega)$ cannot be expected, so that $L^2(\Omega)$ is not the right choice for the state space. In fact, we will find in Lemma 3.9 that $D_s \mathcal{E}(t, \varphi(t), s(t)) := \beta'(s(t))W_1(\mathbb{M}\nabla\varphi(t)) + \omega'(s(t)) - \Delta s(t)$ is bounded only in \mathbf{X}^* the dual of the space $\mathbf{X} := H^1(\Omega) \cap L^\infty(\Omega)$.

In fact, formulation (3.4c) for $\alpha > 0$, i.e. when the unidirectionality constraint is active, corresponds to a one-sided variational inequality. This formulation has also been applied in [HK11] for a damage model in the small-strain setting.

The proof of Thm. 3.10, i.e. of the existence of a solution $(\varphi, s) : [0, T] \rightarrow \mathbf{U} \times \mathbf{Z}$ of $(\mathbf{U} \times \mathbf{Z}, \mathcal{E}, \mathcal{V}_\alpha)$, which satisfies the governing equations (3.4) will be carried out in Section 3.3 using a discretization both in time and in space. For this, we will consider an equidistant partition of the time interval

$$\Pi_N := \{0 = t_N^0 < t_N^1 < \dots < t_N^N = T\} \text{ with time-step size } \tau_N := t_N^i - t_N^{i-1} \rightarrow \text{ as } N \rightarrow \infty. \quad (3.5)$$

In addition, for the analysis, we will also regularize the unidirectionality constraint $I_{(-\infty,0]}$ by its corresponding Yosida approximation, i.e. for each $N \in \mathbb{N}$ we introduce

$$\mathcal{V}_{\alpha N}(\dot{s}) := \int_{\mathcal{B}_0} \left(\frac{M^{-1}}{2} |\dot{s}|^2 + \alpha \frac{N}{2} |(\dot{s})_+|^2 \right) dX \quad (3.6)$$

where $(\dot{s})_+ := \max\{0, \dot{s}\}$ is the positive part of \dot{s} . Starting out from an admissible initial datum $(\varphi^0, z^0) \in \mathbf{U} \times \mathbf{Z}$, at each time-step $t_N^k \in \Pi_N$ we then solve

$$\varphi_N^k \in \operatorname{argmin}_{\tilde{\varphi} \in \mathbf{U}} \mathcal{E}(t_N^k, \tilde{\varphi}, s_N^{k-1}), \quad (3.7a)$$

$$s_N^k \in \operatorname{argmin}_{\tilde{s} \in \mathbf{Z}} \left(\mathcal{E}(t_N^k, \varphi_N^k, \tilde{s}) + \tau_N \mathcal{V}_{\alpha N} \left(\frac{\tilde{s} - s_N^{k-1}}{\tau_N} \right) \right). \quad (3.7b)$$

Existence of solutions (φ_N^k, s_N^k) of (3.7) at each time-step t_N^k will be shown in Prop. 3.8. Using the discrete solutions $(\varphi_N^k, s_N^k)_{k=1}^N$ we will construct suitable interpolants with respect to time and show in our main result, Thm. 3.10, that these interpolants approximate a solution of the continuous problem

(3.4). In fact, in addition we will also find that solutions of (3.4) obtained in this way, also satisfy an energy dissipation estimate of the form:

$$\mathcal{E}(t, \boldsymbol{\varphi}(t), s(t)) + \int_0^t \mathcal{V}_\alpha(\dot{s}(\tau)) \, d\tau \leq \mathcal{E}(0, \boldsymbol{\varphi}^0, s^0) + \int_0^t \mathcal{P}(\tau, s(\tau)) \, d\tau,$$

with \mathcal{V}_α from (3.3) and with $\mathcal{P}(\tau, s(\tau)) := \sup\{\partial_\tau \mathcal{E}(\tau, \hat{\boldsymbol{\varphi}}, s(\tau)), \hat{\boldsymbol{\varphi}} \in \operatorname{argmin}\mathcal{E}(\tau, \cdot, s(\tau))\}$ as a surrogate for the partial time derivative. This surrogate is due to the non-uniqueness of minimizers for polyconvex energies as they arise in the finite strain setting.

3.1 Analytical Setup: Assumptions and Direct Implications

A physically reasonable deformation preserves orientation, which is ensured by

$$\nabla \boldsymbol{\varphi} \in \operatorname{GL}_+(d) = \{F \in \mathbb{R}^{d \times d} \mid \det F > 0\}.$$

Further natural requirements on the constitutive relations of particular importance are material frame indifference (3.8a) and the non-interpenetration condition (3.8b):

$$\hat{W}(RF) = \hat{W}(F) \quad \text{for } R \in \operatorname{SO}(d), F \in \mathbb{R}^{d \times d}, \quad (3.8a)$$

$$\begin{cases} \hat{W}(F) = +\infty & \text{for } \det F \leq 0, \\ \hat{W}(F) \rightarrow +\infty & \text{for } \det F \rightarrow 0_+, \end{cases} \quad (3.8b)$$

since they are not compatible with convexity, which is a convenient claim in the setting of small strains. To see the incompatibility with convexity consider $P, Q \in \operatorname{SO}(d)$, $\lambda \in (0, 1)$, such that $(\lambda P + (1 - \lambda)Q) \notin \operatorname{SO}(d)$, which conforms to a strain. Then convexity together with material frame indifference yields the following contradiction:

$$0 < \hat{W}(\lambda P + (1 - \lambda)Q) \leq \lambda \hat{W}(P) + (1 - \lambda) \hat{W}(Q) = \lambda \hat{W}(I) + (1 - \lambda) \hat{W}(I) = 0.$$

The class of energy densities which fit to these natural requirements and which admit to prove existence are the polyconvex energy densities. They were introduced by J.M. Ball in [Bal76].

Definition 3.1 (Polyconvexity). *The function $\hat{W} : \mathbb{R}^{d \times d} \rightarrow \mathbb{R}_\infty = \mathbb{R} \cup \{\infty\}$ is called polyconvex if there exists a convex function $\tilde{W} : \mathbb{R}^{\mu_d} \rightarrow \mathbb{R}_\infty$, such that $\hat{W}(F) = \tilde{W}(\mathbb{M}(F))$ for all $F \in \mathbb{R}^{d \times d}$, where*

$$\mathbb{M} : \mathbb{R}^{d \times d} \rightarrow \mathbb{R}^{\mu_d} \quad \text{with} \quad \mu_d = \sum_{s=1}^d \binom{d}{s}^2 \quad (3.9)$$

is the function, which maps a matrix to all its minors.

In [Bal76, p. 362] it was established that the polyconvexity of $\hat{W} : \mathbb{R}^{d \times d} \rightarrow \mathbb{R}$ implies its quasiconvexity. By C.B. Morrey in [Mor52] it was proven that quasiconvexity is the notion of convexity which is necessary and sufficient for the lower semicontinuity of the corresponding integral functionals, so that quasiconvexity together with other technical assumptions ensures the existence of minimizers. But quasiconvexity does not admit infinitely valued functions, i.e. $\hat{W} : \mathbb{R}^{d \times d} \rightarrow \mathbb{R}_\infty$. However in [Bal76, Th. 7.3, p. 376] it was shown that the polyconvexity of the density $\hat{W} : \mathbb{R}^{d \times d} \rightarrow \mathbb{R}_\infty$ together with other technical assumptions is sufficient for the existence of minimizers of infinitely valued functionals. More precisely, for the stored elastic energy density $W : \mathbb{R} \times \mathbb{R}^3 \rightarrow \mathbb{R}$ given by

$$W(\mathbf{F}, s) := \beta(s)W_1(\mathbb{M}\mathbf{F}) + W_2(\mathbb{M}\mathbf{F}) \quad \text{from (3.1) with } \beta : \mathbb{R} \rightarrow [a, \infty) \quad \text{from (3.10g)} \quad (3.10a)$$

we make the following assumptions:

- **Continuity:** $W(\cdot, \cdot) \in C^0(\mathbb{R}^{3 \times 3} \times \mathbb{R}, \mathbb{R})$, (3.10b)

- **Polyconvexity:** $W_1, W_2 : \mathbb{R}^{3 \times 3} \times \mathbb{R}^{3 \times 3} \times \mathbb{R} \rightarrow \mathbb{R}$ are convex. (3.10c)

- **Coercivity:** There are constants $p \geq 2, p_2 \geq \frac{p}{p-1}, p_3 > 1, c_1, c_2, c_3, C > 0$ so that it holds for all

$$(\mathbf{F}, s) \in \mathbb{R}^{3 \times 3} \times \mathbb{R} : c_1 |\mathbf{F}|^p + c_2 |\text{cof} \mathbf{F}|^{p_2} + c_3 |\det \mathbf{F}|^{p_3} - C \leq W(\mathbf{F}, s). \quad (3.10d)$$

- **Stress control:**

For all $s \in \mathbb{R}$ we have $W(\cdot, s) \in C^1(\text{GL}_+(3), \mathbb{R})$ and there are constants $c > 0, \tilde{c} \geq 0$ such that for all $(\mathbf{F}, s) \in \mathbb{R}^{3 \times 3} \times \mathbb{R}$ it holds

$$|\partial_{\mathbf{F}} W(\mathbf{F}, s) \mathbf{F}^\top| \leq c(W(\mathbf{F}, s) + \tilde{c}). \quad (3.10e)$$

- **Uniform continuity of the stresses:**

There is a modulus of continuity $o : [0, \infty] \rightarrow [0, \infty], \delta > 0$ so that for all

$(\mathbf{F}, s) \in \mathbb{R}^{3 \times 3} \times \mathbb{R}$ and all $C \in \text{GL}_+(3)$ with $|C - \text{id}| \leq \delta$ we have

$$|\partial_{\mathbf{F}} W(C\mathbf{F}, s)(C\mathbf{F})^\top - \partial_{\mathbf{F}} W(\mathbf{F}, s) \mathbf{F}^\top| \leq o(|C - \text{id}|)(W(\mathbf{F}, s) + \tilde{c}). \quad (3.10f)$$

- **Definition of β :** $\beta : \mathbb{R} \rightarrow [\eta, \infty), \beta(s) = \eta + s^2$. (3.10g)

The next lemma goes back on [Bal76]. A proof of the version below is given in [FM06].

Lemma 3.2. *Let be satisfied. Then there is $\delta > 0$ so that for all $\mathbf{C} \in \text{GL}_+(3)$ with $|\mathbf{C} - \text{Id}| \leq \delta$ we have*

$$W(\mathbf{C}\mathbf{F}, s) + \tilde{c} \leq \frac{3}{2}(W(\mathbf{F}, s) + \tilde{c}) \quad (3.11)$$

$$|\partial_{\mathbf{F}} W(\mathbf{C}\mathbf{F}, s) \mathbf{F}^\top| \leq 3c(W(\mathbf{F}, s) + \tilde{c}). \quad (3.12)$$

Moreover, for the function $\gamma : \mathbb{R} \rightarrow [0, \infty)$ we assume that

$$\gamma \in C^2(\mathbb{R} \times \mathbb{R}^3, \mathbb{R}), \gamma(s, \nabla s) := \frac{1}{2l_c}(1-s)^2 + \frac{l_c}{2} |\nabla s|^2, \quad (3.13)$$

Now, as in (3.1) we consider a body with reference configuration $\mathcal{B}_0 \subset \mathbb{R}^3$ consisting of a nonlinearly elastic material, such that

$$\mathcal{B}_0 \text{ is a bounded Lipschitz domain, } \partial \mathcal{B}_0^D \subset \partial \mathcal{B}_0 \text{ with } \partial \mathcal{B}_0^D \neq \emptyset, \partial \mathcal{B}_0^N := \partial \mathcal{B}_0 \setminus \partial \mathcal{B}_0^D. \quad (3.14)$$

This body undergoes a damage process driven by time-dependent exterior forces $h(t)$ located on the Neumann part $\partial \mathcal{B}_0^N \subset \partial \mathcal{B}_0$ of the boundary. Moreover, the body is assumed to be clamped at the remaining part $\partial \mathcal{B}_0^D$ of its boundary, so that the deformation is prescribed there: $\varphi(t) = g(t)$ on $\partial \mathcal{B}_0^D$.

Thus, the set of admissible deformations at time $t \in [0, T]$ is given by

$$\mathbf{U}(t) := \{\phi \in W^{1,p}(\Omega, \mathbb{R}^3) \mid \phi = \mathbf{g}(t) \text{ on } \partial \mathcal{B}_0^D\} \quad \text{for } \frac{3}{2} < p < \infty \quad (3.15)$$

with the weak $W^{1,p}$ -topology. Observe that the assumption on the exponent $p \in (3/2, \infty)$ ensures that

$$W^{1,p}(\mathcal{B}_0, \mathbb{R}^3) \Subset L^{p'}(\mathcal{B}_0, \mathbb{R}^3) \text{ compactly, where } p' := \frac{p}{p-1}. \quad (3.16)$$

Adapting the ideas of [FM06] from the setting where $p > 3$ to the present setting $p \in (3/2, \infty)$, we assume that the Dirichlet datum can be extended to \mathbb{R}^3 in the following way:

$$\mathbf{g} \in C^1([0, T] \times \mathbb{R}^3, \mathbb{R}^3), \nabla \mathbf{g} \in \text{BC}^1([0, T] \times \mathbb{R}^3, \text{Lin}(\mathbb{R}^3, \mathbb{R}^3)), \nabla^2 \mathbf{g} \in \text{B}([0, T] \times \mathbb{R}^3, \text{Lin}(\mathbb{R}^{3 \times 3}, \mathbb{R}^{3 \times 3})), \quad (3.17a)$$

$$\text{with } C_{\mathbf{g}} := \sup_{t \in [0, T], y \in \mathbb{R}^3} (|\nabla \mathbf{g}(t, y)| + |\partial_t \nabla \mathbf{g}(t, y)| + |\nabla^2 \mathbf{g}(t, y)|), \quad (3.17b)$$

$$|\mathbf{g}(t, y)| \leq c_{\mathbf{g}}(1 + |y|) \quad \text{for all } (t, y) \in [0, T] \times \mathbb{R}^3, \quad (3.17c)$$

$$|(\nabla \mathbf{g}(t, y))^{-1}| \leq \tilde{C}_{\mathbf{g}} \text{ for all } (t, y) \in [0, T] \times \mathbb{R}^3. \quad (3.17d)$$

For the time-dependent Neumann datum we impose that

$$\mathbf{h} \in C^1([0, T], L^{p'}(\partial\mathcal{B}_0^N, \mathbb{R}^3)) \text{ with } C_{\mathbf{h}} := \|\mathbf{h}\|_{C^1([0, T], L^{p'}(\partial\mathcal{B}_0^N, \mathbb{R}^3))}. \quad (3.18)$$

To handle the time-dependent Dirichlet conditions one assumes that the deformation is of the form

$$\varphi(t, X) = \mathbf{g}(t, y(X)) \text{ with } y \in \mathbf{Y}, \text{ where} \quad (3.19)$$

$$\mathbf{Y} := \{y \in W^{1,p}(\Omega, \mathbb{R}^d) \mid y = \text{id on } \partial\mathcal{B}_0^D\} \text{ for } d < p < \infty \quad (3.20)$$

with the weak $W^{1,p}$ -topology. By the chain rule, this composition leads to a multiplicative split of the deformation gradient:

$$\nabla\varphi(t, x) = \nabla_X \mathbf{g}(t, y(X)) = \nabla_y \mathbf{g}(t, y(X)) \nabla_X y(X) = \nabla \mathbf{g}(t, y) \nabla y.$$

Furthermore, we introduce the space

$$\mathbf{Y}_0 := \mathbf{Y} - \{\text{id}\}. \quad (3.21)$$

Under consideration of (3.1) and the explanations along with (3.4) we choose the set of admissible damage variables \mathbf{Z} in (3.1) and the set of admissible test functions \mathbf{X} in (3.4) as

$$\mathbf{Z} := \{\tilde{s} \in H^1(\mathcal{B}_0), \tilde{s} = 1 \text{ in trace sense}\} \quad (3.22a)$$

$$\mathbf{X} := \mathbf{Z} \cap L^\infty(\mathcal{B}_0) \quad (3.22b)$$

equipped with the respective weak topologies. The sets \mathbf{Y} and \mathbf{Z} form the state space $\mathbf{Y} \times \mathbf{Z}$, which is endowed with the weak topology of the product space.

For the closed subspace $\mathbf{U}_0 \subset W^{1,p}(\mathcal{B}_0, \mathbb{R}^3)$ one can prove Friedrich's inequality by contradiction using that the embedding $W^{1,p}(\mathcal{B}_0, \mathbb{R}^3) \Subset L^p(\mathcal{B}_0, \mathbb{R}^{3 \times 3})$ is compact.

Theorem 3.3 (Friedrich's inequality). *Let $\mathcal{B}_0 \subset \mathbb{R}^3$ be a Lipschitz domain with Dirichlet conditions on $\partial\mathcal{B}_0^D \subset \partial\mathcal{B}_0$, where $\partial\mathcal{B}_0^D \neq \emptyset$. Let $1 < p < \infty$. There is a constant $C_F = C_F(\mathcal{B}_0, p)$ such that the following estimate holds for every $y_0 \in \mathbf{U}_0$:*

$$\|y_0\|_{W^{1,p}(\mathcal{B}_0, \mathbb{R}^3)} \leq C_F \|\nabla y_0\|_{L^p(\mathcal{B}_0, \mathbb{R}^{3 \times 3})}. \quad (3.23)$$

The lemma below is a consequence of the growth restriction (3.17c).

Lemma 3.4. *Let (3.14), (3.17) as well as (3.19) hold. For every $y \in \mathbf{Y}$ and $\varphi(t) = \mathbf{g}(t, y)$ it holds $\|\varphi(t)\|_{W^{1,p}(\mathcal{B}_0, \mathbb{R}^3)}^p \leq \hat{C}_{\mathbf{g}} (\|y\|_{W^{1,p}(\mathcal{B}_0, \mathbb{R}^3)}^p + 1)$*

Proof. By the growth restriction (3.17c) one directly obtains

$$\|\varphi(t)\|_{W^{1,p}(\mathcal{B}_0, \mathbb{R}^3)}^p \leq 2^{p-1} c_{\mathbf{g}}^p (\mathcal{L}^3(\mathcal{B}_0) + \|y\|_{L^p(\mathcal{B}_0, \mathbb{R}^3)}^p) + C_{\mathbf{g}}^p \|\nabla y\|_{L^p(\mathcal{B}_0, \mathbb{R}^{3 \times 3})}^p.$$

Hence $\hat{C}_{\mathbf{g}} := \max\{2^{p-1} c_{\mathbf{g}}^p, C_{\mathbf{g}}^p, 2^{p-1} c_{\mathbf{g}}^p \mathcal{L}^3(\mathcal{B}_0)\}$. □

Lemma 3.5. *Let (3.17), (3.19) and (3.20) hold. Consider a sequence $(y_k)_{k \in \mathbb{N}} \subset \mathbf{Y}$ such that $y_k \rightharpoonup y$ in \mathbf{Y} . Then $\varphi_k(t) = \mathbf{g}(t, y_k) \rightharpoonup \mathbf{g}(t, y) = \varphi(t)$ in $\mathbf{U}(t)$ for all $t \in [0, T]$.*

Proof. We have the compact embeddings $W^{1,p}(\mathcal{B}_0, \mathbb{R}^3) \Subset L^p(\mathcal{B}_0, \mathbb{R}^3)$ and $W^{1,p}(\mathcal{B}_0, \mathbb{R}^3) \Subset L^{p'}(\mathcal{B}_0, \mathbb{R}^3)$ by (3.16) and hence $y_k \rightarrow y$ in both in $L^{p'}(\mathcal{B}_0, \mathbb{R}^3)$ and in $L^p(\mathcal{B}_0, \mathbb{R}^3)$. By (3.17a) & (3.17b) we now find $\|\varphi_k(t) - \varphi(t)\|_{L^p(\mathcal{B}_0, \mathbb{R}^3)} \leq \sup_{\tilde{y} \in \mathbb{R}^3} |\nabla \mathbf{g}(t, \tilde{y})| \|y_k(t) - y(t)\|_{L^p(\mathcal{B}_0, \mathbb{R}^3)} \leq C_{\mathbf{g}} \|y_k(t) - y(t)\|_{L^p(\mathcal{B}_0, \mathbb{R}^3)} \rightarrow 0$ as $k \rightarrow \infty$. Furthermore, we obtain $\nabla \varphi_k(t) \rightharpoonup \nabla \varphi(t)$ in $L^p(\Omega, \mathbb{R}^{d \times d})$, since $\nabla y_k \rightharpoonup \nabla y$ in $L^p(\Omega, \mathbb{R}^{d \times d})$ and $\nabla \mathbf{g}(t, y_k) \rightarrow \nabla \mathbf{g}(t, y)$ in $L^{p'}(\mathcal{B}_0, \mathbb{R}^{3 \times 3})$, which ensues from (3.17b) by $\|\nabla \mathbf{g}(t, y_k) - \nabla \mathbf{g}(t, y)\|_{L^{p'}(\mathcal{B}_0, \mathbb{R}^{3 \times 3})} \leq \sup_{\tilde{y} \in \mathbb{R}^3} |\nabla^2 \mathbf{g}(t, \tilde{y})| \|y_k(t) - y(t)\|_{L^{p'}(\mathcal{B}_0, \mathbb{R}^3)} \leq C_{\mathbf{g}} \|y_k(t) - y(t)\|_{L^{p'}(\mathcal{B}_0, \mathbb{R}^3)} \rightarrow 0$ as $k \rightarrow \infty$. □

Proposition 3.6 (Compactness of minors of gradients according to (3.10d)). *Consider a sequence $(\varphi_k)_k \subset \mathbf{U}$ such that for all $k \in \mathbb{N}$*

$$C \geq c_1 \|\nabla \varphi_k\|_{L^p(\mathcal{B}_0, \mathbb{R}^{3 \times 3})}^p + c_2 \|\text{cof} \nabla \varphi_k\|_{L^{p_2}(\mathcal{B}_0, \mathbb{R}^{3 \times 3})}^{p_2} + c_3 \|\det \nabla \varphi_k\|_{L^{p_3}(\mathcal{B}_0, \mathbb{R})}^{p_3} - C. \quad (3.24)$$

Then there exists a not relabeled subsequence $(\varphi_k)_k \subset \mathbf{U}$ and $\varphi \in \mathbf{U}$ such that $\varphi_k \rightharpoonup \varphi$ in \mathbf{U} , $\text{cof} \nabla \varphi_k \rightharpoonup \text{cof} \nabla \varphi$ in $L^{p_2}(\mathcal{B}_0, \mathbb{R}^3 \times 3)$, and $\det \nabla \varphi_k \rightharpoonup \det \nabla \varphi$ in $L^{p_3}(\mathcal{B}_0, \mathbb{R})$.

Proof. The proof can be retrieved from [Dac89, p. 183]. \square

In the following we prove temporal regularity properties of the energy functional with respect to time, based on assumption (3.17), (3.18) and (3.10). An analogous result was first obtained in [FM06, Lemma 5.5].

Proposition 3.7. *Let (3.17), (3.18), and (3.10) be satisfied. Then there exist constants $c_0 \geq 0, c_1 > 0$ such that for all $(t_*, \mathbf{g}(t_*, y), s) \in [0, T] \times \mathbf{U} \times \mathbf{Z}$ with $\mathcal{E}(t_*, \mathbf{g}(t_*, y), s) < \infty$ it holds: $\mathcal{E}(\cdot, \mathbf{g}(\cdot, y), s) \in C^1([0, T])$ with*

$$\partial_t \mathcal{E}(t, q) = \int_{\mathcal{B}_0} \partial_F W(F(t), s) F^\top : G(t) - \langle \dot{l}(t), \varphi(t) \rangle - \langle l(t), \partial_t \varphi(t) \rangle \quad (3.25)$$

for $F(t) := \nabla \varphi(t)$ and $G(t) := (\nabla \mathbf{g}(t, y))^{-1} \partial_t \nabla \mathbf{g}(t, y)$ and

$$|\partial_t \mathcal{E}(t, \mathbf{g}(t, y), s)| \leq c_1 (\mathcal{E}(t, \mathbf{g}(t, y), s) + c_0) \quad \text{for every } t \in [0, T]. \quad (3.26)$$

Moreover, the following Lipschitz-estimate holds true:

$$|\mathcal{E}(t, \mathbf{g}(t, y), s) - \mathcal{E}(\tau, \mathbf{g}(\tau, y), s)| \leq c_E |t - \tau|. \quad (3.27)$$

Proof. We confine ourselves to prove the existence of $\partial_t \mathcal{E}(\cdot, q)$ and estimate (3.26) in a neighborhood $\mathcal{N}(t_q)$ of $t_q \in [0, T]$. Similarly to the small-strain setting, where an analogous proof was carried out in [TM10, Thm. 3.7], this is basically done with the mean value theorem of differentiability and the dominated convergence theorem. But the different treatment of the inhomogeneous Dirichlet condition requires different estimates, which will be carried out here. The existence of $\partial_t \mathcal{E}(\cdot, q)$ and the validity of (3.26) on the whole interval $[0, T]$ can then be concluded with the same arguments as in the proof of [TM10, Thm. 3.7].

Since $\partial_t \int_{\Gamma_N} \mathbf{h}(t) \varphi(t) \, d\mathcal{H}^2$ exists by (3.17) & (3.18), it remains to show the existence of $\partial_t \int_{\mathcal{B}_0} W(\nabla \varphi(t)) \, dX$ in $\mathcal{N}(t_q)$. For this we define for $t \in \mathcal{N}(t_q)$

$$h(x, t, \alpha) := \begin{cases} \frac{1}{\alpha} (W(\nabla \varphi(t+\alpha), s) - W(\nabla \varphi(t), s)) & \text{if } \alpha \neq 0 \\ \partial_F W(\nabla \varphi(t), s) (\nabla \varphi(t))^\top : (\nabla \mathbf{g}(t, y))^{-1} \partial_t \nabla \mathbf{g}(t, y) & \text{if } \alpha = 0 \end{cases}$$

and we have to show that $h(x, t, \cdot) \in C^0([-\alpha_t, \alpha_t])$ for α_t suitably. By the mean value theorem of differentiability we find $\tilde{\alpha} = \tilde{\alpha}(\alpha)$ such that it holds for every $\alpha \in [-\alpha_t, \alpha_t]$

$$\begin{aligned} & \frac{1}{\alpha} (W(\nabla \varphi(t+\alpha), s) - W(\nabla \varphi(t), s)) \\ &= \partial_F W(\nabla \varphi(t+\tilde{\alpha}), s) (\nabla \varphi(t+\tilde{\alpha}))^\top : (\nabla \mathbf{g}(t+\tilde{\alpha}, y))^{-1} \partial_t \nabla \mathbf{g}(t+\tilde{\alpha}, y) \\ & \rightarrow \partial_F W(\nabla \varphi(t), s) (\nabla \varphi(t))^\top : (\nabla \mathbf{g}(t, y))^{-1} \partial_t \nabla \mathbf{g}(t, y) \end{aligned} \quad (3.28)$$

as $\alpha, \tilde{\alpha} \rightarrow 0$ by (3.2) and (3.17). In order to show that the integrals converge as well, we are going to apply the dominated convergence theorem. For this, we have to construct an integrable majorant for expression (3.28). Again by the mean value theorem of differentiability we first obtain $\hat{\alpha}$ such that

$$\nabla \varphi(t+\tilde{\alpha}) = \nabla(\varphi(t) + \partial_t \varphi(t+\hat{\alpha}) \tilde{\alpha}) = (\text{Id} + \tilde{\alpha} \partial_t \nabla \mathbf{g}(t+\hat{\alpha}, y) (\nabla \mathbf{g}(t, y))^{-1}) \nabla \varphi(t) = C(\tilde{\alpha}) \nabla \varphi(t)$$

with $C(\tilde{\alpha}) \rightarrow \text{Id}$ as $\tilde{\alpha} \rightarrow 0$. Hence we conclude by (3.12) and (3.17):

$$\begin{aligned} |(3.28)| &\leq \tilde{C}_g C_g |\partial_F W(C(\tilde{\alpha}), s)(\nabla \varphi(t))^\top C(\tilde{\alpha})^\top| \\ &\leq \tilde{C}_g C_g dc(W(\nabla \varphi(t), s) + \tilde{c})(\sqrt{d} + \tilde{\alpha} C_g \tilde{C}_g). \end{aligned} \quad (3.29)$$

Now, estimate (3.26) is derived under consideration of

$$|\partial_t \mathcal{E}(t, q)| \leq \left| \int_{\mathcal{B}_0} h(x, t, 0) \right| + |\langle \dot{\mathbf{h}}(t), \varphi(t) \rangle| + |\langle \mathbf{h}(t), \partial_t \varphi(t) \rangle|. \quad (3.30)$$

In view of (3.17), (3.18), Lemma 3.4, Friedrich's inequality (3.23), Young's inequality and 3.10d we derive for the loading terms in (3.30) an estimate of the form

$$|\langle \dot{\mathbf{h}}(t), \varphi(t) \rangle| + |\langle \mathbf{h}(t), \partial_t \varphi(t) \rangle| \leq A_1 \mathcal{E}(t, q) + B_1.$$

For the elastic energy term in (3.30) estimate (3.29) and (3.17), (3.18) lead to

$$\left| \int_{\mathcal{B}_0} h(x, t, 0) \right| \leq (3.29) \leq A_2 \mathcal{E}(t, q) + B_2,$$

so that inequality (3.26) is obtained. \square

3.2 Analytical Results on Convergence Properties

In this section we gather and explain all our analytical results.

In a first step we verify the existence of discrete solutions $(\varphi_N^k, s_N^k) \in \mathbf{U} \times \mathbf{Z}$ at each time-step $t_N^k \in \Pi_N$.

Proposition 3.8 (Existence of solutions for the discrete problem (3.7)). *Let the assumptions (3.10), (3.18), (3.17) & (3.14) hold true and $(\mathbf{U} \times \mathbf{Z}, \mathcal{E}, \mathcal{V}_{\alpha N})$ be given by (3.1), (3.6), (3.15), (3.22a). Consider a partition Π_N of $[0, T]$ as in (3.5). Suppose that $(y^0, s^0) \in \mathbf{Y} \times \mathbf{Z}$ is an admissible initial datum. Then, the following statements hold true for each $t_N^k \in \Pi_N$ as in (3.5):*

1. *There exists a pair $(y_N^k, s_N^k) \in \mathbf{Y} \times \mathbf{Z}$ such that $(\varphi(t_N^k, y_N^k), s_N^k) \in \mathbf{U} \times \mathbf{Z}$ is a solution for minimization problem (3.7).*
2. *Let the initial datum $(y^0, s^0) \in \mathbf{Y} \times \mathbf{Z}$ such that $s^0 \in [0, 1]$ a.e. on \mathcal{B}_0 . Then, a solution s_N^k of (3.7b) also satisfies $s_N^k \in [0, 1]$ a.e. in \mathcal{B}_0 both for $\alpha = 0$ and for $\alpha > 0$ in (3.6), i.e. $s_N^k \in \mathbf{X} = H^1(\mathcal{B}_0) \cap L^\infty(\mathcal{B}_0)$.*

Using the discrete solutions $(y_N^k, s_N^k)_{k=1}^N$ obtained in Prop. 3.8 we now introduce piecewise constant left-continuous (\bar{y}_N, \bar{s}_N) (right-continuous $(\underline{y}_N, \underline{s}_N)$) piecewise constant interpolants and linear interpolants s_N^ℓ as follows:

$$(\bar{y}_N(t), \bar{s}_N(t)) := (y_N^k, s_N^k) \text{ for all } t \in (t_N^{k-1}, t_N^k], \quad (3.31a)$$

$$(\underline{y}_N(t), \underline{s}_N(t)) := (y_N^{k-1}, s_N^{k-1}) \text{ for all } t \in [t_N^{k-1}, t_N^k), \quad (3.31b)$$

$$s_N^\ell := \frac{t - t_N^{k-1}}{\tau_N} s_N^k + \frac{t_N^k - t}{\tau_N} s_N^{k-1} \quad (3.31c)$$

and accordingly, we set $\bar{\varphi}_N(t) := \bar{\mathbf{g}}(t, \bar{y}_N(t))$ and $\underline{\varphi}_N(t) := \underline{\mathbf{g}}(t, \underline{y}_N(t))$.

For the interpolants $(\bar{y}_N, \underline{y}_N, \bar{s}_N, \underline{s}_N, s_N^\ell)$ we then verify that they satisfy a discrete version of the governing equations (3.4) and uniform apriori estimates.

Proposition 3.9 (Properties of the interpolants $(\bar{y}_N, \underline{y}_N, \bar{s}_N, \underline{s}_N, s_N^\ell)$). *Let the assumptions of Prop. 3.8 hold true with $s_N^0 \in [0, 1]$ a.e. in \mathcal{B}_0 . Then the interpolants $(\bar{y}_N, \underline{y}_N, \bar{s}_N, \underline{s}_N, s_N^\ell)$ constructed from solutions $(y_N^k, s_N^k)_{k=1}^N$ of problem (3.7) via (3.31) satisfy uniformly for all $N \in \mathbb{N}$:*

$$\text{For all } \tilde{\varphi} \in \mathbf{U}(t) : \mathcal{E}(t, \bar{\varphi}_N(t), \underline{s}_N(t)) \leq \mathcal{E}(t, \tilde{\varphi}, \underline{s}_N(t)), \quad (3.32a)$$

$$D_s \mathcal{E}(t, \bar{\varphi}_N(t), \bar{s}_N(t)) + \tau_N D \mathcal{V}_{\alpha N}(\dot{s}_N^\ell(t)) = 0 \text{ in } \mathbf{X}^*, \text{ i.e., for all } \tilde{s} \in \mathbf{X} : \quad (3.32b)$$

$$\int_{\mathcal{B}_0} \left((\beta'(\bar{s}_N(t)) W_1(\mathbb{M} \nabla \bar{\varphi}_N(t))) - \frac{1}{l_c} (1 - \bar{s}_N) + M^{-1} \dot{s}_N^\ell + \alpha N (\dot{s}_N^\ell)_+ \right) \tilde{s} + l_c \nabla \bar{s}_N(t) : \nabla \tilde{s} \Big) dX = 0.$$

In addition, the following energy-dissipation estimate holds true for all $N \in \mathbb{N}$ and $t \in [0, T]$:

$$\mathcal{E}(t, \bar{\varphi}_N(t), \bar{s}_N(t)) + \int_0^t \mathcal{V}_{\alpha N}(\dot{s}_N^\ell(\tau)) \, d\tau \leq \mathcal{E}(0, \varphi_N^0, s_N^0) + \int_0^t \partial_\tau \mathcal{E}(\tau, \mathbf{g}(\tau, \underline{y}_N(\tau)), \underline{s}_N(\tau)) \, d\tau, \quad (3.33)$$

where the partial time derivative $\partial_\tau \mathcal{E}(\tau, \mathbf{g}(\tau, \underline{y}_N(\tau)), \underline{s}_N(\tau))$ is given by (3.25).

Furthermore, there is a constant $C > 0$ such that the following apriori estimates are satisfied uniformly for all $N \in \mathbb{N}$ and all $t \in [0, T]$:

$$\mathcal{E}(t, \bar{\varphi}_N(t), \bar{s}_N(t)) \leq C, \quad \mathcal{E}(t, \underline{\varphi}_N(t), \underline{s}_N(t)) \leq C, \quad \int_0^t \mathcal{V}_{\alpha N}(\dot{s}_N^\ell(\tau)) \, d\tau \leq C, \quad (3.34a)$$

$$\|\bar{y}_N(t)\|_{\mathbf{Y}} \leq C \quad \& \quad \|\underline{y}_N(t)\|_{\mathbf{Y}} \leq C, \quad (3.34b)$$

$$\|\dot{s}_N^\ell\|_{L^2(0, t; L^2(\mathcal{B}_0))} \leq C, \quad (3.34c)$$

$$\|\bar{s}_N(t)\|_{\mathbf{Z}} \leq C \quad \& \quad \|\underline{s}_N(t)\|_{\mathbf{Z}} \leq C, \quad (3.34d)$$

$$\|\bar{s}_N(t)\|_{L^\infty(\mathcal{B}_0)} \leq 1 \quad \& \quad \|\underline{s}_N(t)\|_{L^\infty(\mathcal{B}_0)} \leq 1, \quad (3.34e)$$

$$\|\beta(\bar{s}_N(t)) W_1(\mathbb{M}\nabla \bar{\varphi}_N(t))\|_{\mathbf{X}^*} \leq C. \quad (3.34f)$$

Thanks to the apriori estimates (3.34) we are now in the position to extract a (not relabeled) subsequence $(\bar{y}_N, \underline{y}_N, \bar{s}_N, \underline{s}_N, \dot{s}_N^\ell)_N$ of the interpolants, which converge to a limit pair (y, s) that satisfies (3.4):

Theorem 3.10 (Convergence of the time-discrete solutions, existence of a solution for (3.4)). *Let the assumptions of Prop. 3.9 hold true. Then there is a (not relabeled) subsequence $(\bar{y}_N, \underline{y}_N, \bar{s}_N, \underline{s}_N, \dot{s}_N^\ell)_N$ satisfying (3.32)–(3.34), a function $\underline{y} : [0, T] \rightarrow \mathbf{Y}$, and a pair $(y, s) : [0, T] \rightarrow \mathbf{Y} \times \mathbf{X}$ with $\varphi(t) = \mathbf{g}(t, y(t))$ such that*

$$s_N^\ell \rightharpoonup s \text{ in } H^1(0, T; L^2(\mathcal{B}_0)), \quad (3.35a)$$

$$s_N^\ell, \bar{s}_N, \underline{s}_N \rightharpoonup s \text{ in } L^2(0, T; L^2(\mathcal{B}_0)), \quad (3.35b)$$

$$\bar{s}_N(t), \underline{s}_N(t) \rightharpoonup s(t) \text{ in } \mathbf{X} \text{ for all } t \in [0, T], \quad (3.35c)$$

$$\bar{y}_N(t) \rightharpoonup y(t) \text{ in } \mathbf{Y} \text{ for a.a. } t \in (0, T), \quad (3.35d)$$

$$\underline{y}_N(t) \rightharpoonup \underline{y}(t) \text{ in } \mathbf{Y} \text{ for a.a. } t \in (0, T), \quad (3.35e)$$

$$W_i(\mathbb{M}\nabla \bar{\varphi}_N(t)) \rightharpoonup W_i(\mathbb{M}\nabla \varphi(t)) \text{ in } L^1(\mathcal{B}_0) \text{ for a.a. } t \in (0, T), \quad i = 1, 2. \quad (3.35f)$$

In particular, the pair $(y, s) : [0, T] \rightarrow \mathbf{Y} \times \mathbf{X}$ satisfies:

- For all $t \in [0, T]$, for all $\tilde{\varphi} \in \mathbf{U}$: $\mathcal{E}(t, \varphi(t), s(t)) \leq \mathcal{E}(t, \tilde{\varphi}, s(t))$, (3.36a)

- if $\alpha = 0$, for a.a. $t \in (0, T)$, for all $\tilde{s} \in \mathbf{X}$: (3.36b)

$$\int_{\mathcal{B}_0} \left((\beta'(s(t)) W_1(\mathbb{M}\nabla \varphi(t))) - \frac{1}{l_c} (1 - s(t)) + M^{-1} \dot{s}(t) \tilde{s} + l_c \nabla s(t) : \nabla \tilde{s} \right) \, dX = 0,$$

- if $\alpha > 0$, for a.a. $t \in (0, T)$, for all $\tilde{s} \in \mathbf{X}$ such that $\tilde{s} \leq 0$ a.e. in \mathcal{B}_0 : (3.36c)

$$\int_{\mathcal{B}_0} \left((\beta'(s(t)) W_1(\mathbb{M}\nabla \varphi(t))) - \frac{1}{l_c} (1 - s(t)) + M^{-1} \dot{s}(t) \tilde{s} + l_c \nabla s(t) : \nabla \tilde{s} \right) \, dX \geq 0,$$

- if $\alpha > 0$, then $\dot{s}(t) \leq 0$ for a.a. $t \in (0, T)$, a.e. in \mathcal{B}_0 , (3.36d)

- and the energy dissipation inequality for all $t \in [0, T]$: (3.36e)

$$\mathcal{E}(t, \varphi(t), s(t)) + \int_0^t \mathcal{V}_\alpha(\dot{s}(\tau)) \, d\tau \leq \mathcal{E}(0, \varphi^0, s^0) + \int_0^t \mathcal{P}(\tau, s(\tau)) \, d\tau,$$

with \mathcal{V}_α from (3.3) and with $\mathcal{P}(\tau, s(\tau)) := \sup\{\partial_\tau \mathcal{E}(\tau, \hat{\varphi}, s(\tau)), \hat{\varphi} \in \operatorname{argmin}\mathcal{E}(\tau, \cdot, s(\tau))\}$ as a surrogate for the partial time derivative from (3.25).

3.3 Proofs of Prop. 3.8–Thm. 3.10

3.3.1 Proof of Prop. 3.8

In order to establish the proof of Item 1, we will employ the direct method of the calculus of variations. For this, we will verify the coercivity and the weak sequential lower semicontinuity of the functional $\mathcal{E}(t, \cdot, \cdot)$. To deduce the latter for the polyconvex functional $\mathcal{E}(t, \cdot, \cdot)$ we use the following result on the convergence of minors of gradients, which goes back on [Res67, Bal76], cf. also [MM09]. With this at hand we now establish weak sequential lower semicontinuity and coercivity.

Lemma 3.11. *Let (3.14), (3.17), (3.18) as well as (3.10a)–(3.10d) hold. Then, for all $t \in [0, T]$ the following statements hold true:*

1. $\mathcal{E}(t, \cdot, \cdot)$ is coercive on $\mathbf{U} \times \mathbf{Z}$ for all $t \in [0, T]$, in particular, there are constants $B, C > 0$ such that for all $(y, s) \in \mathbf{Y} \times \mathbf{Z}$ with $\varphi = \mathbf{g}(t, y)$ it holds:

$$\mathcal{E}(t, \varphi, s) \leq C(\|y\|_{W^{1,p}(\mathcal{B}_0, \mathbb{R}^3)}^p + \|\operatorname{cof} \nabla \varphi\|_{L^{p_2}(\mathcal{B}_0, \mathbb{R}^{3 \times 3})}^{p_2} + \|\det \nabla \varphi\|_{L^{p_3}(\mathcal{B}_0, \mathbb{R})}^3) + \frac{l_c}{2} \|s\|_{H^1(\mathcal{B}_0)}^2 - B. \quad (3.37)$$

2. $\mathcal{E}(t, \cdot, \cdot) : \mathbf{U} \times \mathbf{Z} \rightarrow \mathbb{R}$ has weakly sequentially compact sublevels.

Proof. Proof of 1.: Let $(y_k, s_k)_{k \in \mathbb{N}} \subset \mathbf{Y} \times \mathbf{Z}$. By (2.3), (3.10d), (3.17), (3.18), Young's inequality with $\varepsilon = (\frac{c_1 p}{2C_g^p C_F^p})^{\frac{1}{p}}$, Lemma 3.4 and Friedrich's inequality it is:

$$\begin{aligned} & \mathcal{E}(t, \varphi_k, s_k) \\ & \geq (c_1 \|\nabla \varphi_k(t)\|_{L^p(\Omega, \mathbb{R}^{3 \times 3})}^p + c_2 \|\operatorname{cof} \nabla \varphi_k\|_{L^{p_2}(\mathcal{B}_0, \mathbb{R}^{3 \times 3})}^{p_2} + c_3 \|\det \nabla \varphi_k\|_{L^{p_3}(\mathcal{B}_0, \mathbb{R})}^3 - C \mathcal{L}^3(\mathcal{B}_0) \\ & \quad + \frac{l_c}{2} \|s\|_{H^1(\mathcal{B}_0)}^2 - \frac{1}{2l_c} \mathcal{L}^3(\mathcal{B}_0) - \left(\frac{C_h}{p'\varepsilon}\right)^{p'} - \frac{\varepsilon^p}{p} \|\varphi_k(t)\|_{W^{1,p}(\mathcal{B}_0, \mathbb{R}^3)}^p) \\ & \geq \left(\frac{c_1}{C_g^p} (2^{1-p} \|\nabla(y_k - \operatorname{id})\|_{L^p(\mathcal{B}_0, \mathbb{R}^{3 \times 3})}^p - 3^{\frac{1}{p}} \mathcal{L}^3(\mathcal{B}_0)) + c_2 \|\operatorname{cof} \nabla \varphi_k\|_{L^{p_2}(\mathcal{B}_0, \mathbb{R}^{3 \times 3})}^{p_2} \right. \\ & \quad \left. + c_3 \|\det \nabla \varphi_k\|_{L^{p_3}(\mathcal{B}_0, \mathbb{R})}^3 - C \mathcal{L}^3(\mathcal{B}_0) + \frac{l_c}{2} \|s\|_{H^1(\mathcal{B}_0)}^2 - \frac{\varepsilon^p}{p} (\|y_k\|_{W^{1,p}(\mathcal{B}_0, \mathbb{R}^3)}^p + 1) - \tilde{B}\right) \\ & \geq \left(\frac{c_1}{C_g^p C_F^p} - \frac{\varepsilon^p}{p}\right) \|y_k\|_{W^{1,p}(\mathcal{B}_0, \mathbb{R}^3)}^p + c_2 \|\operatorname{cof} \nabla \varphi_k\|_{L^{p_2}(\mathcal{B}_0, \mathbb{R}^{3 \times 3})}^{p_2} + c_3 \|\det \nabla \varphi_k\|_{L^{p_3}(\mathcal{B}_0, \mathbb{R})}^3 + \frac{l_c}{2} \|s_k\|_{H^1(\mathcal{B}_0)}^2 - B, \end{aligned}$$

which states (3.37).

Proof of 2.: To establish the weak sequential compactness of the energy sublevels we now consider a sequence $(y_k, s_k)_{k \in \mathbb{N}} \subset \mathbf{Y} \times \mathbf{Z}$ with $\mathcal{E}(t, \varphi_k, s_k) \leq C$ uniformly for all $k \in \mathbb{N}$. Coercivity estimate (3.37) thus allows us to employ Prop. 3.6, which implies the existence of a subsequence $y_k \rightharpoonup y$ in \mathbf{Y} , such that $\varphi_k \rightharpoonup \varphi$ in \mathbf{U} , $\operatorname{cof} \nabla \varphi_k \rightharpoonup \operatorname{cof} \nabla \varphi$ in $L^{p_2}(\mathcal{B}_0, \mathbb{R}^{3 \times 3})$, and $\det \nabla \varphi_k \rightharpoonup \det \nabla \varphi$ in $L^{p_3}(\mathcal{B}_0, \mathbb{R})$. Moreover, we also find a subsequence $s_k \rightharpoonup s$ in \mathbf{Z} . It thus remains to deduce the weak sequential lower semicontinuity of each of the contributions of \mathcal{E} .

To establish the weak sequential lower semicontinuity of the functional $\int_{\mathcal{B}_0} \gamma(\cdot, \cdot) dX : \mathbf{Z} \times \mathbf{Z} \rightarrow [0, \infty)$ with γ from (2.3). We first note that $\gamma \in C^1(\mathbb{R} \times \mathbb{R}^3, \mathbb{R})$ and bounded from below by 0. Moreover, the gradient term is strictly convex and the compact embedding $\mathbf{Z} \Subset L^2(\Omega)$ will ensure that $s_k \rightarrow s$ strongly in $L^2(\mathcal{B}_0)$ if $s_k \rightharpoonup s$ in \mathbf{Z} . Hence, the weak sequential lower semicontinuity of the integral functional follows by [Dac89, Sec. 3, Thm. 3.4].

Assumption (3.18) and Lemma 3.5 ensure that $\int_{\partial \mathcal{B}_0^N} \mathbf{h}(t), \mathbf{g}(t, y_k) dX \rightarrow \int_{\partial \mathcal{B}_0^N} \mathbf{h}(t), \mathbf{g}(t, y) dX$. Further taking into account Hypotheses (3.10b)–(3.10d), which state that W is a Carathéodory-function, polyconvex and bounded from below for every $\mathbf{F} \in \operatorname{GL}_+(3)$, the weak sequential lower semicontinuity of $\int_{\mathcal{B}_0} g(\cdot) W_1(\mathbb{M}(\cdot)) + W_2(\mathbb{M}(\cdot)) dX$ can be obtained by applying weak lower semicontinuity results for the convex case, cf. [Dac89, Sec. 3, Thm. 3.4]. \square

We are now in the position to verify the existence of minimizers for problem (3.4) via the direct method of the calculus of variations.

Proof of Prop. 3.8, Item 1: Asume that $s_N^0 \in [0, 1]$ a.e. in \mathcal{B}_0 . Thus, $\mathcal{E}(t_N^1, \cdot, s_N^0) : \mathbf{U} \rightarrow \mathbb{R}$ is well-defined. We conclude the existence of a minimizer $y_N^1 \in \mathbf{Y}_N$ such that $\varphi_N^1 = \mathbf{g}(t_N^1, y_N^1)$ via the direct

method of the calculus of variations by applying Lemma 3.11 to $\mathcal{E}(t_N^1, \cdot, s_N^0)$. Let $t_N^k \in \Pi_N$ fixed and assume that $s_N^1 \in [0, 1]$ (which we will show in Item 2 by induction). Again, $\mathcal{E}(t_N^k, \cdot, s_N^{k-1}) : \mathbf{U} \rightarrow \mathbb{R}$ is well-defined and we may deduce the existence of a minimizer $y_N^k \in \mathbf{Y}_N$ such that $\varphi_N^k = \mathbf{g}(t_N^k, y_N^k)$ via the direct method by applying Lemma 3.11 to $\mathcal{E}(t_N^k, \cdot, s_N^{k-1})$. Similarly, the existence of a minimizer s_N^k follows from Lemma 3.11 applied to the functional $\mathcal{E}(t_N^k, \varphi_N^k, \cdot) + \tau_N \mathcal{V}_{\alpha N}(\frac{\cdot - s_N^{k-1}}{\tau_N})$. For this, note that $\mathcal{V}_{\alpha N}(\frac{\cdot - s_N^{k-1}}{\tau_N})$ only contains quadratic, convex lower order terms. \blacksquare

Proof of Prop. 3.8, Item 2: We proceed by contradiction. For this, suppose that $s_N^{k-1} \in [0, 1]$ a.e. in \mathcal{B}_0 but that there exist sets $B^0, B^1 \subset \mathcal{B}_0$ with $\mathcal{L}^3(B^0), \mathcal{L}^3(B^1) > 0$ such that $s_N^k < 0$ a.e. on B^0 and $s_N^k > 1$ a.e. on B^1 . We test the minimality (3.7b) by $\tilde{s} := \min\{1, \max\{0, s_N^k\}\}$. In view of (3.10g), (3.13), (3.1), and (3.6) we thus have

$$\begin{aligned} \beta(s_N^k)W_1(\mathbb{M}\nabla\varphi_N^k) &\geq \beta(\tilde{s})W_1(\mathbb{M}\nabla\varphi_N^k), \\ (1 - s_N^k)^2 &\geq (1 - \tilde{s})^2, \\ \int_{\mathcal{B}_0} |\nabla s_N^k| dX &\geq \int_{\mathcal{B}_0} |\nabla \tilde{s}| dX, \\ \mathcal{V}_{\alpha N}(\frac{s_N^k - s_N^{k-1}}{\tau_N}) &\geq \mathcal{V}_{\alpha N}(\frac{\tilde{s} - s_N^{k-1}}{\tau_N}). \end{aligned}$$

Here, the first inequality follows from the monotonicity of β on $[0, \infty)$ and $(-\infty, 0]$. To see the second inequality observe that $(1 - s)^2 > 1 = (1 - \tilde{s})^2$ for $s < 0$ and $(1 - s)^2 > 0 = (1 - \tilde{s})^2$ for $s > 1$. The third inequality follows from [MM79, Sec. 2], which implies that $\nabla \tilde{s} = 0$ on $B = B^0 \cup B^1$ and $\nabla \tilde{s} = \nabla s_N^k$ on $\mathcal{B}_0 \setminus B$. The fourth inequality ensues from

$$\begin{aligned} \text{for } s_N^k < 0, s_N^{k-1} \geq 0 : & \left(\frac{s_N^k - s_N^{k-1}}{\tau_N}\right)^2 \geq \left(\frac{-s_N^{k-1}}{\tau_N}\right)^2 \ \& \ 0 = \left(\frac{s_N^k - s_N^{k-1}}{\tau_N}\right)_+^2 \geq \left(\frac{-s_N^{k-1}}{\tau_N}\right)_+^2 = 0, \\ \text{for } s_N^k > 1, s_N^{k-1} \leq 1 : & \left(\frac{s_N^k - s_N^{k-1}}{\tau_N}\right)^2 \geq \left(\frac{s_N^{k-1} - 1}{\tau_N}\right)^2 \ \& \ \left(\frac{s_N^k - s_N^{k-1}}{\tau_N}\right)_+^2 \geq \left(\frac{-s_N^{k-1}}{\tau_N}\right)_+^2. \end{aligned}$$

Alltogether, the four relations imply

$$\mathcal{E}(t_N^k, \varphi_N^k, \tilde{s}) + \mathcal{V}_{\alpha N}(\frac{\tilde{s} - s_N^{k-1}}{\tau_N}) < \mathcal{E}(t_N^k, \varphi_N^k, s_N^k) + \mathcal{V}_{\alpha N}(\frac{s_N^k - s_N^{k-1}}{\tau_N}),$$

which is in contradiction to the minimality (??) of s_N^k and hence $s_N^k \in [0, 1]$ a.e. in \mathcal{B}_0 .

Note that the above contradiction argument holds in particular for $k = 1$ under the assumption that $s_N^0 \in [0, 1]$ a.e. in \mathcal{B}_0 , i.e., in this case we find that $s_N^1 \in [0, 1]$ a.e.. Therefore, the above argument allows us to conclude the statement by induction. \blacksquare

3.3.2 Proof of Prop. 3.9

We start with the proof of the discrete notion of solution (3.32).

Proof of (3.32a): We observe that a minimizer φ_N^k of problem (3.7a) equivalently satisfies for all $\tilde{\varphi} \in \mathbf{U}$

$$\mathcal{E}(t_N^k, \varphi_N^k, s_N^{k-1}) \leq \mathcal{E}(t_N^k, \tilde{\varphi}, s_N^{k-1}). \quad (3.38)$$

Applying the definition of the interpolants (3.31) we find (3.32a).

Proof of (3.32b): We use that a minimizer s_N^k of problem (3.7b) satisfies the corresponding Euler-Lagrange equations for all $\tilde{s} \in \mathbf{X}$:

$$\int_{\mathcal{B}_0} \left((\beta'(s_N^k)W_1(\mathbb{M}\nabla\varphi_N^k(t_N^k))) - \frac{1}{l_c}(1 - s_N^k) + M^{-1}\left(\frac{s_N^k - s_N^{k-1}}{\tau_N}\right) + \alpha N\left(\frac{s_N^k - s_N^{k-1}}{\tau_N}\right)_+ \right) \tilde{s} + l_c \nabla s_N^k : \nabla \tilde{s} \Big) dX = 0.$$

Again using the definition of the interpolants (3.31) we find (3.32b).

Proof of (3.33): In order to find the energy dissipation estimate we test the minimality of s_N^k in (3.7b) by s_N^{k-1} , exploit the minimality of y_N^k , and add and subtract $\mathcal{E}(t_N^{k-1}, \varphi_N^{k-1}, s_N^{k-1})$,

$$\begin{aligned} & \mathcal{E}(t_N^k, \varphi_N^k, s_N^k) + \tau_N \mathcal{V}_{\alpha N} \left(\frac{s_N^k - s_N^{k-1}}{\tau_N} \right) \leq \mathcal{E}(t_N^k, \varphi_N^k, s_N^{k-1}) \\ & \leq \mathcal{E}(t_N^k, \varphi_N^{k-1}, s_N^{k-1}) + \mathcal{E}(t_N^{k-1}, \varphi_N^{k-1}, s_N^{k-1}) - \mathcal{E}(t_N^{k-1}, \varphi_N^{k-1}, s_N^{k-1}) \\ & = \mathcal{E}(t_N^k, \varphi_N^{k-1}, s_N^{k-1}) + \int_{t_N^{k-1}}^{t_N^k} \partial_\tau \mathcal{E}(\tau, \mathbf{g}(\tau, y_N^{k-1}), s_N^{k-1}) \, d\tau. \end{aligned} \quad (3.39)$$

Consider now $t \in (t_N^{m-1}, t_N^m]$. Then summing up the above relation over $k \in \{1, \dots, m\}$, results in

$$\mathcal{E}(t_N^m, \varphi_N^m, s_N^m) + \sum_{k=1}^m \tau_N \mathcal{V}_{\alpha N} \left(\frac{s_N^k - s_N^{k-1}}{\tau_N} \right) \leq \mathcal{E}(t_N^0, \varphi_N^0, s_N^0) + \sum_{k=1}^m \int_{t_N^{k-1}}^{t_N^k} \partial_\tau \mathcal{E}(\tau, \mathbf{g}(\tau, y_N^{k-1}), s_N^{k-1}) \, d\tau.$$

Again by the definition of the interpolants and using that $t \in (t_N^{m-1}, t_N^m]$ we see that this relation is equivalent to (3.33).

Proof of (3.34): We now want to exploit the previously obtained discrete estimate (3.39)–(3.33) to deduce the a priori estimates (3.34). To do so, we apply (3.26) under the integral of (3.39). This allows us to apply the classical Gronwall inequality and, following the arguments of e.g. [FM06], one finds for every $m \in \{1, \dots, N\}$

$$\mathcal{E}(t_N^m, \varphi_N^m, s_N^m) + \sum_{k=1}^m \mathcal{V}_{\alpha N} \left(\frac{s_N^k - s_N^{k-1}}{\tau_N} \right) \leq C. \quad (3.40)$$

This translates into (3.34a) and, thanks to (3.37), also yields the estimates (3.34b)–(3.34d). Moreover, in view of $s_N^0 \in [0, 1]$, estimate (3.34e) is due to Prop. 3.8, Item 2. Now, thanks to the properties of β and W_1, W_2 , cf. (3.10g) & (3.10), and coercivity estimate (3.37) we can verify that there is a constant $c_1, c_2 > 0$ such that for all $\bar{s} \in \mathbf{X}$ we have

$$\left| \int_{\mathcal{B}_0} \beta'(\bar{s}_N(t)) W_1(\mathbb{M}\nabla \bar{\varphi}_N(t)) \bar{s} \, dX \right| \leq \|\bar{s}\|_{\mathbf{X}} (c_1 \mathcal{E}(t, \bar{\varphi}_N(t), \bar{s}_N(t)) + c_2).$$

This proves (3.34f). ■

3.3.3 Proof of Theorem 3.10

Proof of convergences (3.35): In view of (3.34c) we find subsequence and a limit $s \in H^1(0, T; L^2(\mathcal{B}_0))$ such that (3.35a) holds true. Similarly, by (3.34d) & (3.34e) we find further subsequences and $\bar{s}, \underline{s} \in \mathbf{X}$, such that also $\bar{s} \xrightarrow{*} \bar{s}$ and $\underline{s} \xrightarrow{*} \underline{s}$ in $L^\infty(0, T; \mathbf{X})$. Since $s_N^\ell(t) - \bar{s}_N(t) = (t - t_N^k) \dot{s}_N^\ell(t)$ and $s_N^\ell(t) - \underline{s}_N(t) = (t - t_N^{k-1}) \dot{s}_N^\ell(t)$, we deduce from convergence (3.35a) that in fact $s = \bar{s} = \underline{s}$ in $L^\infty(0, T; H^1(\mathcal{B}_0))$. This proves convergences (3.35b) & (3.35c) due to the pointwise bounds in time (3.34d) & (3.34e). Convergences (3.35d) & (3.35e) also follow by the boundedness in $L^\infty(0, T; \mathbf{Y})$ implied by the pointwise in time bounds (3.34b). Observe that (3.35d) only holds on $(0, T) \setminus \mathbb{N}$ with $\mathcal{L}^3(\mathbb{N}) = 0$. We can define $y(t)$ for $t \in \mathbb{N}$ by choosing $y(t) \in \mathbf{Y}$ such that $\varphi(t) = \mathbf{g}(t, y(t)) \in \operatorname{argmin}_{\varphi \in \mathbf{U}(t)} \mathcal{E}(t, \tilde{\varphi}, s(t))$. Moreover, it has to be noted that, due to polyconvexity, i.e., the lack of (strict) convexity the uniqueness of minimizers is not guaranteed. This is why $y(t)$ and $\underline{y}(t)$ must not coincide.

It remains to verify the convergence of $W_i(\mathbb{M}\nabla \bar{\varphi}_N(t))$, i.e., (3.35f). For this we test the minimality of $\bar{\varphi}_N(t)$ in (3.32a) by the limit $\varphi(t)$ at any time $t \in (0, T)$, where (3.35d) holds true. Based on this we

argue that

$$\begin{aligned}
& \limsup_{N \rightarrow \infty} \int_{\mathcal{B}_0} (\beta(\underline{s}_N(t))W_1(\mathbb{M}\nabla\bar{\varphi}_N(t)) + W_2(\mathbb{M}\nabla\bar{\varphi}_N(t))) \, dX \\
& \leq \int_{\mathcal{B}_0} (\beta(s(t))W_1(\mathbb{M}\nabla\varphi(t)) + W_2(\mathbb{M}\nabla\varphi(t))) \, dX \\
& \quad + \limsup_{N \rightarrow \infty} \int_{\partial\mathcal{B}_0^N} \mathbf{h} \cdot (\varphi(t) - \varphi_N(t)) \, dX + \limsup_{N \rightarrow \infty} \int_{\mathcal{B}_0} (\beta(\bar{s}_N(t)) - \beta(s(t)))W_1(\mathbb{M}\nabla\varphi(t)) \, dX \\
& = \int_{\mathcal{B}_0} (\beta(s(t))W_1(\mathbb{M}\nabla\varphi(t)) + W_2(\mathbb{M}\nabla\varphi(t))) \, dX.
\end{aligned} \tag{3.41}$$

Here, the convergence of the Neumann boundary-term follows by weak strong convergence arguments taking into account (3.35d) and Prop. 3.6. The convergence of $(\beta(\bar{s}_N(t)) - \beta(s(t)))W_1(\mathbb{M}\nabla\varphi(t)) \rightarrow 0$ in $L^1(\mathcal{B}_0)$ ensues by the dominated convergence theorem, using that convergence (3.35c) implies convergence in measure and that $(1 + \eta)W_1(\mathbb{M}\nabla\varphi(t)) + W_2(\mathbb{M}\nabla\varphi(t))$ provides a majorant. Since all terms are non-negative and $\beta(\cdot)\eta > 0$, estimate (3.41) implies that also

$$\limsup_{N \rightarrow \infty} \int_{\mathcal{B}_0} (W_1(\mathbb{M}\nabla\bar{\varphi}_N(t)) + W_2(\mathbb{M}\nabla\bar{\varphi}_N(t))) \, dX \leq \int_{\mathcal{B}_0} (W_1(\mathbb{M}\nabla\varphi(t)) + W_2(\mathbb{M}\nabla\varphi(t))) \, dX. \tag{3.42}$$

On the other hand, we also have by lower semicontinuity

$$\liminf_{N \rightarrow \infty} \int_{\mathcal{B}_0} (W_1(\mathbb{M}\nabla\bar{\varphi}_N(t)) + W_2(\mathbb{M}\nabla\bar{\varphi}_N(t))) \, dX \geq \int_{\mathcal{B}_0} (W_1(\mathbb{M}\nabla\varphi(t)) + W_2(\mathbb{M}\nabla\varphi(t))) \, dX. \tag{3.43}$$

Hence, (3.35f) is proven.

Proof of the minimality condition (3.36a): Thanks to convergence (3.35d) we find by Prop. 3.6 the weak convergences of the corresponding minors. Additionally, convergence (3.35b) yields the strong convergence $\underline{s}_N(t) \rightarrow s(t)$ in $L^2(\mathcal{B}_0)$ for all $t \in [0, T]$, which in turn implies convergence in measure. Using that $\int_{\mathcal{B}_0} (\beta(\underline{s}_N(t))W_1(\mathbb{M}\nabla\varphi(t)) + W_2(\mathbb{M}\nabla\varphi(t))) \, dx \leq \int_{\mathcal{B}_0} (W_1(\mathbb{M}\nabla\varphi(t)) + W_2(\mathbb{M}\nabla\varphi(t))) \, dx$ we have found a convergent majorant, which allows us to pass to the limit on the right-hand side of (3.32a) by continuity. In turn, the limit passage on the left-hand side of (3.32a) is done by weak lower semicontinuity. This proves (3.36a).

Proof of the evolution equation (3.36b) for $\alpha = 0$: Let now $\alpha = 0$ and we want to show (3.36b). In view of convergences (3.35), we may apply weak-strong convergence arguments to pass to the limit in (3.32b) as an equality, i.e., we find for a.e. $t \in (0, T)$, for every $\tilde{s} \in \mathbf{X}$

$$\int_{\mathcal{B}_0} \left((\beta'(s(t))W_1(\mathbb{M}\nabla\varphi(t)))(t) - \frac{1}{l_c}(1 - s(t)) + M^{-1}\dot{s} \right) \tilde{s} + l_c \nabla s(t) : \nabla \tilde{s} \, dX = 0. \tag{3.44}$$

More precisely, to obtain the first term we apply the dominated convergence theorem arguing that $\beta'(\bar{s}_N(t))W_1(\mathbb{M}\nabla\bar{\varphi}_N(t))\tilde{s} \rightarrow s(t)W_1(\mathbb{M}\nabla\varphi(t))\tilde{s}$ in measure, thanks to (3.35c) & (3.35f), and that $W_1(\mathbb{M}\nabla\bar{\varphi}_N(t))|\tilde{s}|$ provides a convergent majorant for $\tilde{s} \in \mathbf{X}$.

Proof of the evolution equation (3.36c) for $\alpha > 0$: Let now $\alpha > 0$. To show the validity of (3.36c) we observe that $\alpha N(\dot{s}_N^\ell)_+ \tilde{s} \leq 0$ for every $\tilde{s} \in \mathbf{X}$ with $\tilde{s} \leq 0$ a.e. in \mathcal{B}_0 . Hence, when moving this term to the other side of the equation, we find that (3.32b) can be reformulated as a variational inequality, i.e., for all $\tilde{s} \in \mathbf{X}$ with $\tilde{s} \leq 0$ a.e. in \mathcal{B}_0 :

$$0 \leq \int_{\mathcal{B}_0} \left((\beta'(\bar{s}_N(t))W_1(\mathbb{M}\nabla\bar{\varphi}_N(t))) - \frac{1}{l_c}(1 - \bar{s}_N) + M^{-1}\dot{s}_N^\ell \right) \tilde{s} + l_c \nabla \bar{s}_N(t) : \nabla \tilde{s} \, dX. \tag{3.45}$$

We can then pass to the limit on the right-hand side of (3.45) using convergences (3.35) and weak-strong convergence arguments and arguing by dominated convergence for the first term, as in the case $\alpha = 0$.

Proof of nonpositivity (3.36d) if $\alpha > 0$: From the third bound in (3.34a), we gather that

$$\int_0^T \int_{\mathcal{B}_0} (\dot{s}_N^\ell)_+ \, dX \, dt \leq \frac{C}{\alpha N} \rightarrow 0 \text{ as } N \rightarrow \infty.$$

By weak lower semicontinuity and convergence (3.35a) we conclude that

$$0 = \liminf_{N \rightarrow \infty} \int_0^T \int_{\mathcal{B}_0} (\dot{s}_N^\ell)_+ \, dX \, dt \geq \int_0^T \int_{\mathcal{B}_0} (\dot{s})_+ \, dX \, dt,$$

which implies that $\dot{s} \leq 0$ a.e. in $(0, T)$, a.e. in \mathcal{B}_0 .

Proof of the energy-dissipation estimate (3.36f): Thanks to convergences (3.35) we can pass to the limit on the left-hand side of the discrete energy-dissipation estimate (3.33) by lower semicontinuity arguments, also using in the case $\alpha > 0$ that $\mathcal{V}_{\alpha N}(\dot{s}_N^\ell(t)) \geq \mathcal{V}_0(\dot{s}_N^\ell(t))$ and $\mathcal{V}_\alpha(\dot{s}(t)) = \mathcal{V}_0(\dot{s}(t))$ since $\dot{s}(t) \leq 0$ for a.e. $t \in (0, T)$ by (3.36d). On the right-hand side, the energy at initial time is constant wrt. $N \in \mathbb{N}$ and we only have to take care about the limit passage in the powers of the external loadings. For this, we want to show that

$$\limsup_{N \rightarrow \infty} \int_0^t \partial_\tau \mathcal{E}(\tau, \underline{\varphi}_N(\tau), \underline{s}_N(\tau)) \, d\tau \leq \int_0^t \mathcal{P}(\tau, s(\tau)) \, d\tau, \quad (3.46)$$

where $\mathcal{P}(\tau, s(\tau)) := \sup\{\partial_\tau \mathcal{E}(\tau, \tilde{\varphi}, s(\tau)), \tilde{\varphi} \in \operatorname{argmin} \mathcal{E}(\tau, \cdot, s(\tau))\}$ is introduced as a surrogate for the partial time derivative from (3.25). We can conclude (3.46) if we first show that

$$\underline{\varphi}(\tau) \text{ is a minimizer of } \mathcal{E}(\tau, \cdot, s(\tau)) \quad (3.47)$$

and secondly verify that

$$\int_0^t \partial_\tau \mathcal{E}(\tau, \underline{\varphi}_N(\tau), \underline{s}_N(\tau)) \, d\tau \rightarrow \int_0^t \partial_\tau \mathcal{E}(\tau, \underline{\varphi}(\tau), s(\tau)) \, d\tau. \quad (3.48)$$

Clearly, these two properties imply (3.46) due to the definition of \mathcal{P} . In addition, by the power control estimate (3.26), we see that $\int_0^t \mathcal{P}(\tau, s(\tau)) \, d\tau$ is well-defined and finite.

We now prove statement (3.47). For this, we introduce a further interpolant, i.e.

$$\underline{s}_N(t) := s_N^{k-1} \text{ for all } t \in [t_N^k, t_N^{k+1}) \text{ for } k \in \{1, \dots, N\}, \underline{s}_N(t) := s_N^0 \text{ for all } t \in [t_N^0, t_N^1), \quad (3.49)$$

which thus satisfies $\underline{s}_N(t) = \underline{s}_N(t - \tau_N) = \bar{s}_N(t - 2\tau_N)$ for $t \in [t_N^k, t_N^{k+1})$ and all $k \in \{1, \dots, N\}$. With similar arguments as for the proof of convergences (3.35b) & (3.35c) we find that

$$\underline{s}_N(t) \xrightarrow{*} s(t) \text{ in } L^\infty(0, T; \mathbf{X}). \quad (3.50)$$

Using the interpolant \underline{s}_N , we can rewrite minimality condition (3.38) for all $\tilde{\varphi} \in \mathbf{U}(\underline{t}_N(t))$ as

$$\mathcal{E}(\underline{t}_N(t), \underline{\varphi}_N(t), \underline{s}_N(t)) \leq \mathcal{E}(\underline{t}_N(t), \tilde{\varphi}, \underline{s}_N(t)). \quad (3.51)$$

Using convergences (3.35e) & (3.50) and by repeating the arguments of the proof of minimality condition (3.36a) we conclude (3.47).

We now turn to the proof of the convergence of the powers of the energy (3.46). For this, we will adapt the arguments of [Tho10, Sec. 3] and [FM06, Prop. 3.3] to the present, rate-dependent situation. More precisely, for $\mathcal{J} : [0, T] \times \mathbf{U} \times \mathbf{Z}$, $\mathcal{J}(t, \varphi, s) := \int_{\mathcal{B}_0} W(\nabla \varphi, s) \, dX - \int_{\partial \mathcal{B}_0^N} \mathbf{h} \cdot \varphi \, dX$ we shall show in Lemma 3.12 below that

1. It holds $\mathcal{J}(t, \varphi_m, s_m) \rightarrow \mathcal{J}(t, \varphi, s)$ for every sequence $s_m \rightarrow s$ in \mathbf{X} and $\varphi_m \rightarrow \varphi$ in \mathbf{U} such that $\varphi_m \in \operatorname{argmin}\{\mathcal{J}(t_m, \tilde{\varphi}, s_m), \tilde{\varphi} \in \mathbf{U}\}$.
2. For every pair (y, s) such that $\mathcal{E}(0, \mathbf{g}(0, y), s) < E$ the derivative $\partial_t \mathcal{E}(\cdot, \mathbf{g}(\cdot, y), s) = \partial_t \mathcal{J}(\cdot, \mathbf{g}(\cdot, y), s)$ is uniformly continuous.

The lower semicontinuity of $\mathcal{J}(t, \cdot, \cdot)$ in $\mathbf{U} \times \mathbf{Z}$ together with the above Items 1& 2 will allow us to apply [FM06, Prop. 3.3], which then implies that $\partial_t \mathcal{J}(t, \varphi_m, s_m) \rightarrow \partial_t \mathcal{J}(t, \varphi, s)$. In other words, this result allows us to conclude that $\partial_\tau \mathcal{E}(\tau, \underline{\varphi}(\tau), \underline{s}(\tau)) \rightarrow \partial_\tau \mathcal{E}(\tau, \varphi(\tau), s(\tau))$ pointwise in $\tau \in [0, T]$. Using again the power control (3.26) providing an integrable majorant, the dominated convergence theorem yields statement (3.48). Hence the upper energy-dissipation estimate (3.36f) is proven, so that the proof of Thm. 3.10 is concluded. \blacksquare

We now provide the following result, which was used for the proof of the upper energy dissipation estimate (3.36f):

Lemma 3.12 (Convergence of the energies and powers). *Let the assumptions of Thm. 3.10 be satisfied and denote $\mathcal{J} : [0, T] \times \mathbf{U} \times \mathbf{Z}$, $\mathcal{J}(t, \boldsymbol{\varphi}, s) := \int_{\mathcal{B}_0} W(\nabla \boldsymbol{\varphi}, s) dX - \int_{\partial \mathcal{B}_0^N} \mathbf{h} \cdot \boldsymbol{\varphi} dX$. Then, the following statements hold true:*

1. *It holds $\mathcal{J}(t, \boldsymbol{\varphi}_m, s_m) \rightarrow \mathcal{J}(t, \boldsymbol{\varphi}, s)$ for every sequence $s_m \rightarrow s$ in \mathbf{X} and $\boldsymbol{\varphi}_m \rightarrow \boldsymbol{\varphi}$ in \mathbf{U} such that $\boldsymbol{\varphi}_m \in \operatorname{argmin}\{\mathcal{J}(t_m, \tilde{\boldsymbol{\varphi}}, s_m), \tilde{\boldsymbol{\varphi}} \in \mathbf{U}\}$.*
2. *For every pair (y, s) such that $\mathcal{E}(0, \mathbf{g}(0, y), s) < E$ the derivative $\partial_t \mathcal{E}(\cdot, \mathbf{g}(\cdot, y), s) = \partial_t \mathcal{J}(\cdot, \mathbf{g}(\cdot, y), s)$ is uniformly continuous, i.e., for each $E, \varepsilon > 0$ there is $\delta > 0$ such that for all (y, s) with $\mathcal{E}(0, \mathbf{g}(0, y), s) < E$ it is*

$$|\partial_t \mathcal{J}(t, \mathbf{g}(\cdot, y), s) - \partial_t \mathcal{J}(\tau, \mathbf{g}(\cdot, y), s)| < \varepsilon \quad \text{if } |t - \tau| < \delta. \quad (3.52)$$

Proof. We start with the proof Item 1. Consider a sequence $s_m \rightarrow s$ in \mathbf{X} with $\|s_m\|_{L^\infty(\mathcal{B}_0)} \leq 1$ and $y \in \mathbf{X}$ such that $\mathcal{E}(0, \mathbf{g}(0, y), s_1) < E$. Then we find that $\mathcal{J}(t, \mathbf{g}(t, y), s_m) \rightarrow \mathcal{J}(t, \mathbf{g}(t, y), s)$. Note that the convergence of the Neumann boundary terms is due to the assumptions (3.17) & (3.18). Moreover, the convergence of the bulk term follows from the dominated convergence theorem, since $W(t, \mathbf{g}(t, y), s_m) \rightarrow W(t, \mathbf{g}(t, y), s)$ in measure thanks to convergence (3.35c) and since $W(t, \mathbf{g}(t, y), 1)$ provides an integrable majorant. Moreover, $\boldsymbol{\varphi}_m$ minimizes $\mathcal{J}(t_m, \cdot, s_m)$. Hence, by assumptions (3.17) & (3.18) there is a constant E such that $\mathcal{J}(t, \boldsymbol{\varphi}_m, s_m) < E$ for all $t \in [0, T]$. Thus (3.27) holds and we infer

$$\mathcal{J}(t, \boldsymbol{\varphi}_m, s_m) - c_E |t_m - t| \leq \mathcal{J}(t_m, \boldsymbol{\varphi}_m, s_m) \leq \mathcal{J}(t, \boldsymbol{\varphi}, s_m) + c_E |t_m - t| \rightarrow \mathcal{J}(t, \boldsymbol{\varphi}, s)$$

We conclude $\mathcal{J}(t_m, \boldsymbol{\varphi}_m, s_m) \rightarrow \mathcal{J}(t, \boldsymbol{\varphi}, s)$ exploiting the weak sequential lower semicontinuity

$$\begin{aligned} \mathcal{J}(t, \boldsymbol{\varphi}, s) &\leq \liminf_{m \rightarrow \infty} (\mathcal{J}(t, \boldsymbol{\varphi}_m, s_m) - c_E |t_m - t|) \leq \liminf_{m \rightarrow \infty} \mathcal{J}(t_m, \boldsymbol{\varphi}_m, s_m) \\ &\leq \limsup_{m \rightarrow \infty} \mathcal{J}(t_m, \boldsymbol{\varphi}_m, s_m) \leq \limsup_{m \rightarrow \infty} (\mathcal{J}(t, \boldsymbol{\varphi}, s_m) + c_E |t_m - t|) = \mathcal{J}(t, \boldsymbol{\varphi}, s). \end{aligned}$$

Hence Item 1 of the Lemma is verified.

We now prove Item 2. Consider (y, s) such that $\mathcal{E}(0, \mathbf{g}(0, y), s) < E$. Due to (3.17) and (3.18) we find for every $\tilde{\varepsilon} > 0$ a $\tilde{\delta} > 0$ such that for all $\tau, t \in [0, T]$ with $|\tau - t| < \tilde{\delta}$ we have $\|g(\tau, y) - g(t, y)\|_{C^1(\mathcal{B}_0, \mathbb{R}^3)} + \|\dot{g}(\tau, y) - \dot{g}(t, y)\|_{C^1(\mathcal{B}_0, \mathbb{R}^3)} < \tilde{\varepsilon}$. Choose now $\varepsilon, E > 0$. By estimate (3.37) we obtain for $t = 0$:

$$\|y\|_{W^{1,p}(\mathcal{B}_0, \mathbb{R}^3)} \leq \left(\frac{\mathcal{E}(0, \mathbf{g}(0, y), s) + C_3}{c_3} \right)^{\frac{1}{p}} \leq \left(\frac{E + C_3}{c_3} \right)^{\frac{1}{p}} =: \tilde{B}.$$

Thanks to the growth control (3.17c) for \mathbf{g} this shows that $\mathbf{g}(t, y)$ for (y, s) with bounded energy at initial time are uniformly bounded for every $t \in [0, T]$.

Furthermore we estimate

$$\begin{aligned} &|\partial_t \mathcal{J}(t, \mathbf{g}(t, y), s) - \partial_t \mathcal{J}(\tau, \mathbf{g}(\tau, y), s)| \\ &\leq \left| \int_{\mathcal{B}_0} \partial_F W(\nabla \mathbf{g}(t, y), s) (\nabla \mathbf{g}(t, y))^\top : \nabla (\dot{\mathbf{g}}(t, y) - \dot{\mathbf{g}}(\tau, y)) dX \right| \end{aligned} \quad (3.53)$$

$$+ \left| \int_{\mathcal{B}_0} (\partial_F W(\nabla \mathbf{g}(t, y), s) (\nabla \mathbf{g}(t, y))^\top - \partial_F W(\nabla \mathbf{g}(\tau, y), s) (\nabla \mathbf{g}(\tau, y))^\top) : \nabla \dot{\mathbf{g}}(\tau, y) dX \right| \quad (3.54)$$

$$+ \left| \int_{\partial \mathcal{B}_0^N} (\dot{\mathbf{h}}(t) - \dot{\mathbf{h}}(\tau)) \cdot \mathbf{g}(t, y) dX \right| + \left| \int_{\partial \mathcal{B}_0^N} \dot{\mathbf{h}}(\tau) \cdot (\mathbf{g}(t, y) - \mathbf{g}(\tau, y)) dX \right| \quad (3.55)$$

$$+ \left| \int_{\partial \mathcal{B}_0^N} (\mathbf{h}(t) - \mathbf{h}(\tau)) \cdot \dot{\mathbf{g}}(t, y) dX \right| + \left| \int_{\partial \mathcal{B}_0^N} \mathbf{h}(\tau) \cdot (\dot{\mathbf{g}}(t, y) - \dot{\mathbf{g}}(\tau, y)) dX \right|, \quad (3.56)$$

where, thanks to assumptions (3.17) & (3.18), each of the terms in (3.55) & (3.56) can be estimated from above by $\varepsilon/8$ for $|t - \tau| < \tilde{\delta}_0$ sufficiently small.

In view of (3.10d), (3.2) and Lipschitz estimate (3.27) we see that

$$\begin{aligned} (3.53) &\leq \|\partial_F W(\nabla \mathbf{g}(\cdot, y), s) (\nabla \mathbf{g}(\cdot, y))^\top\|_{L^1(\mathcal{B}_0)} \|\nabla (\dot{\mathbf{g}}(t, y) - \dot{\mathbf{g}}(\tau, y))\|_{L^\infty(\mathcal{B}_0, \mathbb{R}^{3 \times 3})} \\ &\leq (\mathcal{E}(0, \mathbf{g}(0, y), s) + C \mathcal{L}^3(\mathcal{B}_0) + c_E T + c_l B) \|\nabla (\dot{\mathbf{g}}(t, y) - \dot{\mathbf{g}}(\tau, y))\|_{L^\infty(\mathcal{B}_0, \mathbb{R}^{3 \times 3})} < \frac{\varepsilon}{4}, \end{aligned}$$

if $|t-\tau| < \tilde{\delta}_1$ is sufficiently small. In view of (3.10f) and the Gronwall estimate we find

$$(3.54) \leq c_g \omega(\|\nabla(\dot{\mathbf{g}}(t, y) - \dot{\mathbf{g}}(\tau, y))\|_{L^\infty}) (\|W(\nabla \mathbf{g}(t, y), s)\|_{L^1} (1 + \exp(2cc_g)) + C) < \frac{\varepsilon}{4}$$

for $|\tau-t| < \tilde{\delta}_2$ sufficiently small, where we used $C := (1 + \exp(2cc_g)cc_g)\tilde{c}\mathcal{L}^d(\Omega)$. Hence we obtain (3.54) $< \frac{\varepsilon}{4}$ if $|s-t| < \tilde{\delta}_2$. Altogether we conclude that $|\partial_t J(s, q) - \partial_t J(t, q)| < \varepsilon$ if $|s-t| < \delta := \min\{\tilde{\delta}_0, \tilde{\delta}_1, \tilde{\delta}_2\}$. \square

4 Numerical Examples

In this section we demonstrate the robustness of the proposed model and the analytical results by a series of numerical examples.

4.1 Mode-I-tension test in two dimensions

As a first numerical example we choose a simple mode-I-tension test in two dimensions and consider a squared plate with a required horizontal notch. The geometry and the related boundary conditions are depicted in the left plot of Fig. 3. At the lower boundary of the plate the displacements are constrained in horizontal and vertical direction and at the upper side prescribed displacements are applied incrementally which are realized by making use of a dirichlet boundary condition. Furthermore, the mesh presented in Fig. 3 is on the basis of the hierarchical refinement strategy ([Hesch15]) and consists of 20×20 quadratic B-splines elements before making use of the refinement. After three local refinement levels in total 2656 elements with overall 12288 degrees of freedom are employed for the tension test.

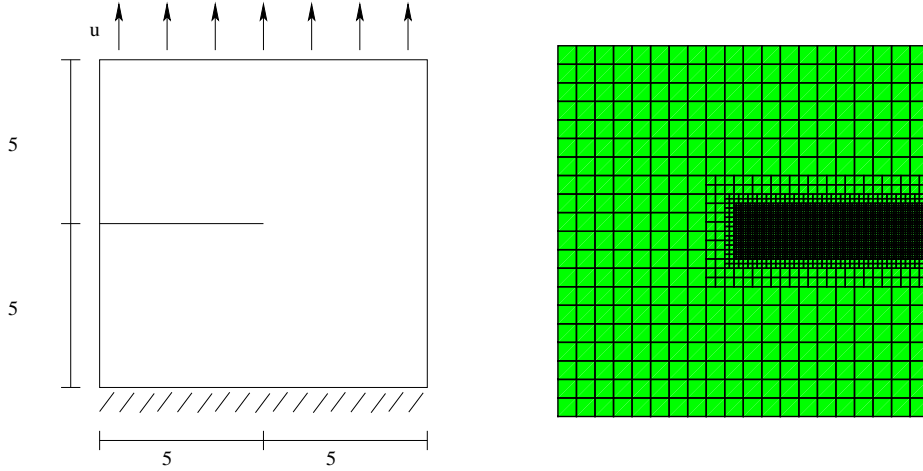


Figure 3: Boundary conditions (left) of a mode-I-tension test and the related mesh based on a hierarchical refinement strategy (right)

The following investigations and simulations are based on the non-linear Neo-Hookean material model which is defined as

$$W(F, J) = \frac{\mu}{2}(I_C - 2) + \frac{\kappa}{2}(J - 1)^2, \quad (4.1)$$

with the shear modulus μ and the bulk modulus κ . Moreover, the proposed anisotropic split (2.11) is applied within this phase-field model. The material parameter are chosen as the Lamé parameters $\lambda = 121.1538 \times 10^9 \frac{\text{N}}{\text{m}^2}$, $\mu = 80.7692 \times 10^9 \frac{\text{N}}{\text{m}^2}$ and the critical energy release rate of $\mathcal{G}_c = 2.7 \times 10^3 \frac{\text{N}}{\text{m}^2}$. On the one hand the related length-scale parameter l_c depends on the mesh size h and has to fulfill the inequality $l_c > 2h$ in general, cf. [Mie10Th], which enables the approximation of a diffuse interface zone. In this case using three level refinements the length scale parameter is set to $l_c = 1.25e - 5$ m. On the

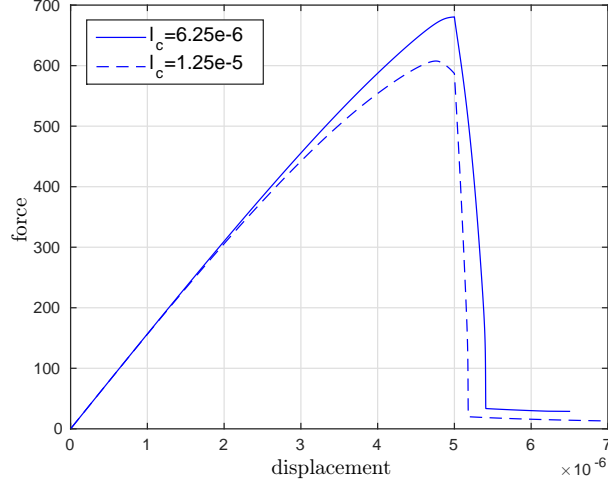


Figure 4: Load-deflection curves for different l_c and the same mesh

other hand l_c operates also as material parameter which can be seen nicely in the load deflection curves in Fig. 4.

The snapshot of the phase-field and the related crack propagation under tension are shown in the left plot of Fig. 5. In order to examine the different solution techniques in more detail, the mode-I-tension test was deduced within the monolithic and the staggered solution scheme. The right plot of Fig. 5 presents the load-deflection curves which show the good accordance of the both solution schemes. However, it can be also seen that the staggered scheme is quite more robust regarding the numerical simulation, because the monolithic curve is aborted earlier.

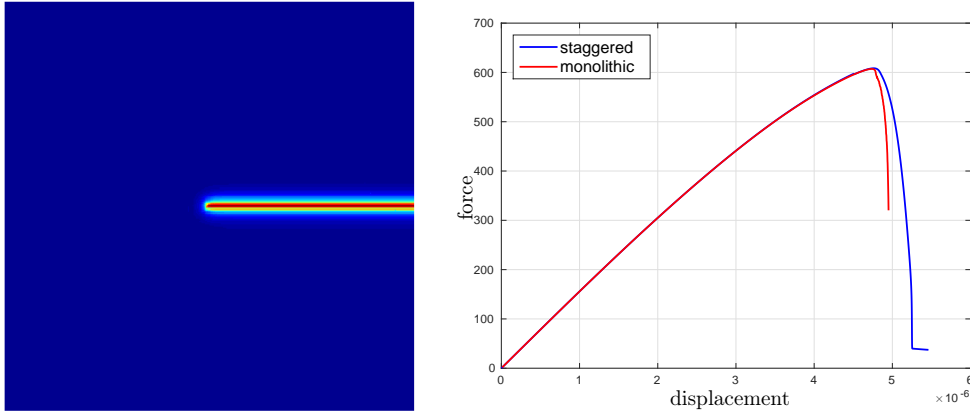


Figure 5: Phase-field snapshot of the mode-I-tension test (left) and load-deflection curves for staggered and monolithic scheme (right)

In a next step the influence of the timestep size is investigated in more detail. The timestep size will be decreased by 0.1 manually during the simulation if the total time of 0.5 sec is achieved. Within this assumption different timestep sizes are examined and the related load-deflection curves are shown in Fig. 6. The results are very similar regarding the crack initialization so that the timestep size do not influence the results in a great measure.

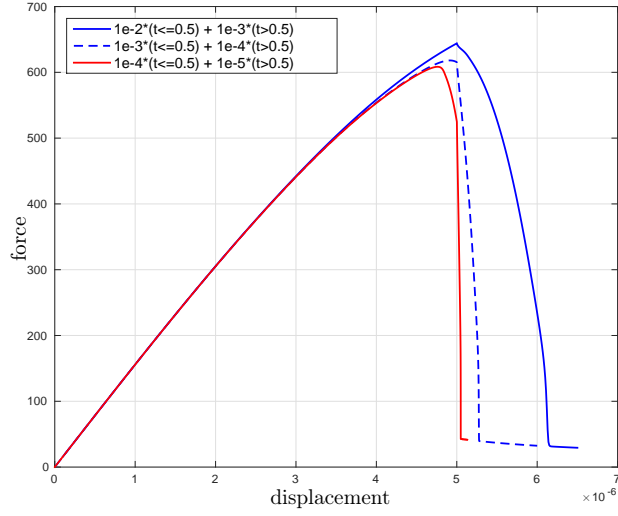


Figure 6: Load-deflection curves for different timestep sizes

4.2 Conchoidal fracture in three dimensions

In this section we simulate a three-dimensional bloc of brittle rock material which is loaded in such a way, that it will crack by conchoidal fracture. The model has been suggested to work as a benchmark problem [Mue2016] in the framework of our DFG Priority Programm 1748.

Conchoidal fracture is a specific type of brittle fracture which is observed in fine-grained or amorphous materials such as rocks, minerals and glasses. Typically it results in a curved breakage surface. Since in conchoidal fracture the shape of the broken surface is controlled only by the stresses state and not by a preferred orientation of the material, the main challenge is to apply a numerical method to predict crack propagation without an initial crack. This type of fracture is often induced by an impact, however, also static loading can induce the mussel shell like shape. Therefore, in the following we employ a quasistatic displacement driven loading regime and the simulation is based on the staggered solution technique.

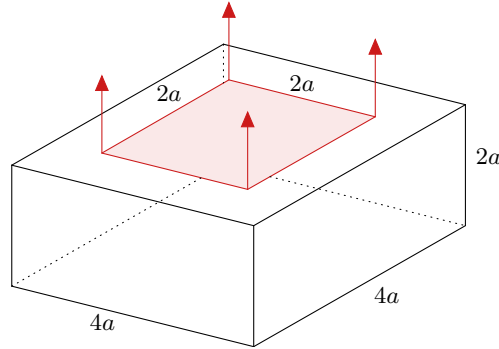


Figure 7: Geometry and loading of a bloc of brittle rock-like material subjected to tension on the upper exterior surface.

We investigate a $4a \times 4a \times 2a$ bloc of stone material subjected to a prescribed displacement on part of its upper boundary, $2a = 1$ m. The geometrical setup of the problem and the boundary conditions are displayed in Fig. 7. On the lower boundary we prescribe Dirichlet conditions $\mathbf{u} = 0$ and $z = 0$ for the displacements and the crack phase field.

In a first step this example is based on the non-linear Neo-Hookean material model

$$W(F, J) = \frac{\mu}{2}(I_C - 3) + \frac{\kappa}{2}(J - 1)^2, \quad (4.2)$$

with the proposed anisotropic split (2.11), the shear modulus μ and the bulk modulus κ whereby the second invariant II_C drops out. The material parameters are chosen as Lamè constant $\lambda = 100000 \text{ N/mm}^2$, shear modulus $\mu = 100000 \text{ N/mm}^2$, and a critical energy release rate of $\mathcal{G}_c = 1 \text{ N/mm}$.

In a second step the Mooney-Rivlin material model is applied to take into account the assumption (3.10d). The related strain energy function is given by

$$W(F, H, J) = c_1(I_C - 3) + c_2(II_C - 3) + \frac{c}{2}(J - 1)^2, \quad (4.3)$$

with the proposed anisotropic split (2.11) and the coefficients $c, c_1, c_2 \in \mathbb{R}^+$. The material parameters are chosen as $c = 1.6667 \times 10^5 \text{ N/mm}^2$, $c_1 = 31000 \text{ N/mm}^2$, $c_2 = 19000 \text{ N/mm}^2$ which correspond to the elasticity modulus $E = 250000 \text{ N/mm}^2$ and poisson ratio $\nu = 0.25$ and a critical energy release rate of $\mathcal{G}_c = 1 \text{ N/mm}$.

The finite element mesh requires a certain minimum element size h in order to resolve the with a length scale parameter of $l_c = 0.2 \text{ m}$. Thus, we discretize the bloc with a structured mesh consisting of 27000 8-node brick elements. The mesh is *not* refined in the area where the crack is expected to propagate — because we do not want to nudge the simulation in any direction.

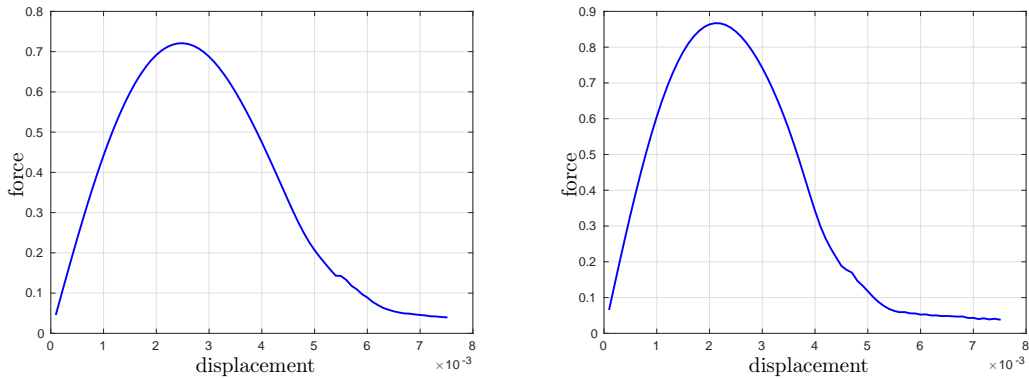


Figure 8: Force-displacement curve obtained for both non-linear elasticity models.

The specimen is subject to a displacement-driven deformation by prescribed incremental displacements of 0.001 mm until crack initiation. The subsequent deformation demands an adjustment of the displacement increments to 0.0001 mm up to the final deformation. The block cracks at a prescribed displacement of about 3 mm approximately, see Fig. 8. The behavior is characterized by a brutal and complete crack growth. In Fig. 9 the crack evolution at different stages of the deformation is displayed for both non-linear models (4.4) and (4.3).

In the non-linear elastic model we find crack initiation inside the bloc below the pulled surface. Please note that the characteristic rippled surface of conchoidal fracture can nicely be observed.

4.3 Brick hole in three dimensions

In the following we investigate a three-dimensional block with a cylindric hole in the middle and of the geometry $50 \times 50 \times 8 \text{ m}$. The geometry and the related mesh with a mesh size of $h = 1 \text{ m}$ are demonstrated in the left plot of Fig. 10 which is based on piecewise Lagrangian polynomials. Furthermore, the upper boundary is loaded by prescribing an incremental displacement whereas the lower boundary is constrained in all directions by applying dirichlet boundary conditions $\varphi = 0$ and $s = 1$ for the displacements and

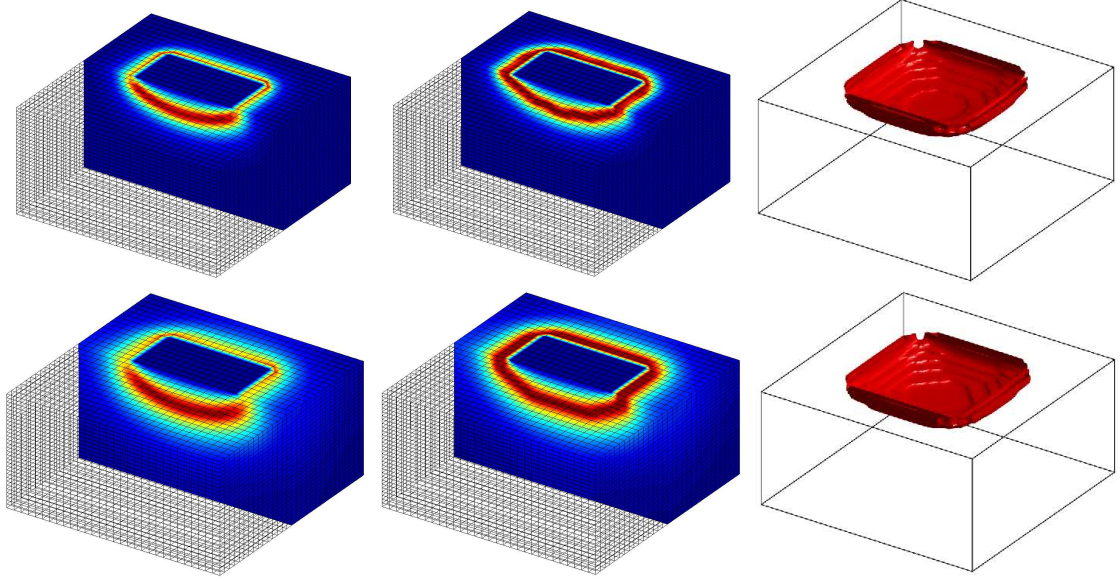


Figure 9: Region of crack initiation, final state and crack surface in the Neo-Hookean (upper row) and Mooney-Rivlin (lower row) model computed with a mesh of $30 \times 30 \times 30$ elements.

the phase-field. The numerical computation is also based on the staggered scheme. This example is also based on the non-linear Neo-Hookean material model in three dimensions

$$W(F, J) = \frac{\mu}{2}(I_C - 3) + \frac{\kappa}{2}(J - 1)^2, \quad (4.4)$$

with the proposed anisotropic split (2.11), the shear modulus μ and the bulk modulus κ . The material parameter are chosen as the Lamè parameters $\lambda = 121.1538 \times 10^9 \frac{\text{N}}{\text{m}^2}$, $\mu = 80.7692 \times 10^9 \frac{\text{N}}{\text{m}^2}$ and the critical energy release rate of $\mathcal{G}_c = 2.7 \times 10^3 \frac{\text{N}}{\text{m}^2}$.

During the simulation it can be observed that the crack propagates horizontally. The results of the phase-field in the current configuration are depicted in the right plot of Fig. 10. Moreover, the block cracks at a prescribed displacement of about 0.017 m, see Fig. 11.

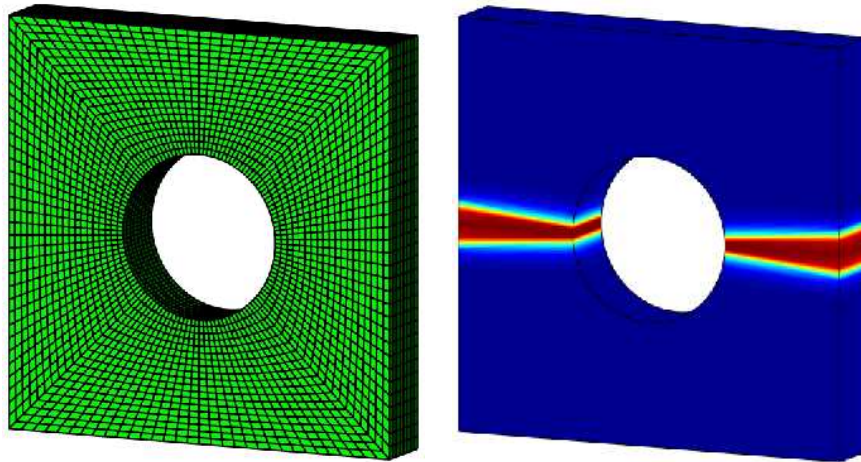


Figure 10: Mesh of the brickhole (left) and phase-field snapshot of the brickhole (right)

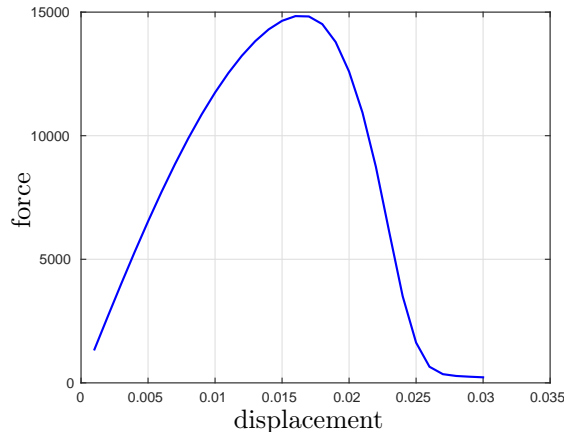


Figure 11: Load-deflection curve of the example brickhole

Acknowledgements: M.T. has been partially supported by the Deutsche Forschungsgemeinschaft in the Priority Program 1748 "Reliable simulation techniques in solid mechanics. Development of non- standard discretization methods, mechanical and mathematical analysis" within the project "Finite element approximation of functions of bounded variation and application to models of damage, fracture, and plasticity". The authors K.W. and C.B. gratefully acknowledge the support of the Deutsche Forschungsgesellschaft (DFG) under the project "Large-scale simulation of pneumatic and hydraulic fracture with a phase-field approach" also as part of the Priority Program SPP 1748 "Reliable simulation techniques in solid mechanics. Development of non- standard discretization methods, mechanical and mathematical analysis"

References

- [Bal76] J. M. Ball. Convexity conditions and existence theorems in nonlinear elasticity. *Arch. Rational Mech. Anal.*, 63(4):337–403, 1976.
- [AT1990] L. Ambrosio and V. M. Tortorelli. Approximation of functionals depending on jumps by elliptic functionals via Γ -convergence. *Comm. Pure Appl. Math.* 43:999–1036, 1990.
- [Bal02] John M. Ball. Some open problems in elasticity. In P. Newton, P. Holmes, and A. Weinstein, editors, *Geometry, Mechanics, and Dynamics*, pages 3–59. Springer, New York, 2002.
- [Bil17] C. Bilgen, A. Kopaničáková, R. Krause and K. Weinberg. A phase-field approach to conchoidal fracture. Submitted to *Meccanica*, 2017
- [Bon15] J. Bonet, A. J. Gil and R. Ortigosa. A computational framework for polyconvex large strain elasticity. *Comput. Methods Appl. Mech. Engrg* 283:1061–1094, 2015.
- [Bor12] M.J. Borden, C.V. Verhoosel, M.A. Scott, T.J.R. Hughes, and C.M. Landis. A phase-field description of dynamic brittle fracture. *Comput. Methods Appl. Mech. Engrg.*, 217–220:77–95, 2012.
- [Dac89] B. Dacorogna. *Direct Methods in the Calculus of Variations*. Springer-Verlag, Berlin, 1989.
- [FM06] G. Francfort and A. Mielke. Existence results for a class of rate-independent material models with nonconvex elastic energies. *J. reine angew. Math.*, 595:55–91, 2006.
- [Gri21] A. A. Griffith. The phenomena of rupture and flow in solids. *Philos. T. R. Soc. Lond.*, 221:163–198, 1921.
- [HK11] C. Heinemann and C. Kraus. Existence of weak solutions for cahn–hilliard systems coupled with elasticity and damage. *Adv. Math. Sci. Appl.*, 21:321–359, 2011.
- [HL04] H. Henry and H. Levine. Dynamic instabilities of fracture under biaxial strain using a phase field model. *Physics Review Letters*, 93:105505, 2004.
- [Hesch15] Christian Hesch, Stefan Schuß, Maik Dittmann, Marlon Franke, Kerstin Weinberg. Isogeometric analysis and hierarchical refinement for higher-order phase-field models. *Computer Methods in Applied Mechanics and Engineering*, 303: 185-207, 2016.

- [Hesch17] C. Hesch, A. J. Gil, R. Ortigosa, M. Dittmann, C. Bilgen, P. Betsch, M. Franke, A. Janz and K. Weinberg. A framework for polyconvex large strain phase-field methods to fracture. *Computer Methods in Applied Mechanics and Engineering* 317:649–683, 2017.
- [Irw58] G. R. Irwin. Elasticity and plasticity: fracture. S. Fürge, editor, *Encyclopedia of Physics*, 1958
- [Kar01] A. Karma, D.A. Kessler, and H. Levine. Phase-field model of mode iii dynamic fracture. *Physical Review Letter*, 81:045501, 2001.
- [Mar03] S. Mariani and U. Perego. Extended finite element method for quasi-brittle fracture. *Int. J. Numer. Meth. Engng*, 58:103–126, 2003.
- [MM79] M. Marcus and V.J. Mizel. Every superposition operator mapping one Sobolev space into another is continuous. *J. Functional Analysis*, 33:217–229, 1979.
- [MM09] A. Mainik and A. Mielke. Global existence for rate-independent gradient plasticity at finite strain. *J. Nonlinear Sci.*, 19(3):221–248, 2009.
- [Mie10PF] C. Miehe, M. Hofacker, and F. Welschinger. A phase field model for rate-independent crack propagation: Robust algorithmic implementation based on operator splits. *Comput. Methods Appl. Mech. Engrg.*, 199:2765–2778, 2010.
- [Mie10Th] C. Miehe, F. Welschinger, and M. Hofacker. Thermodynamically consistent phase-field models of fracture: Variational principles and multi-field fe implementations. *International Journal for Numerical Methods in Engineering*, 83(10): 1273–1311, 2010.
- [Mor52] C. B. Morrey, Jr. Quasi-convexity and the lower semicontinuity of multiple integrals. *Pacific J. Math.*, 2:25–53, 1952.
- [Or99] M. Ortiz and A. Pandolfi. Finite-deformation irreversible cohesive elements for three-dimensional crack-propagation analysis. *International Journal for Numerical Methods in Engineering*, 44(9):1267–1282, 1999.
- [Pan12] A. Pandolfi and M. Ortiz. An eigeneration approach to brittle fracture. *Int. J. Numer. Meth. Engng*, 92:694–714, 2012.
- [Res67] Y.G. Reshetnyak. On the stability of conformal maps in multidimensional spaces. *Siberian Math. J.*, 8:69–85, 1967.
- [Roe03] K.L. Roe and T. Siegmund. An irreversible cohesive zone model for interface fatigue crack growth simulation. *Engineering Fracture Mechanics*, 70(2):209–232, 2003.
- [Schm09] B. Schmidt and S. Leyendecker. Γ -convergence of Variational Integrators for Constraint Systems. *Journal of Nonlinear Science*, 19:153–177, 2009.
- [Suk03] N. Sukumar, D.J. Srolovitz, T.J. Baker and J.-H. Prevost. Brittle fracture in polycrystalline microstructures with the extended finite element method. *Int. J. Numer. Meth. Engng.* 56,2015–2037, 2003.
- [Tho10] M. Thomas. *Rate-independent damage processes in nonlinearly elastic materials*. PhD thesis, Humboldt-Universität zu Berlin, 2010.
- [TM10] M. Thomas and A. Mielke. Damage of nonlinearly elastic materials at small strain: existence and regularity results. *Zeit. angew. Math. Mech.*, 90(2):88–112, 2010.
- [Bor13] C.V. Verhoosel and R. de Borst. A phase-field model for cohesive fracture. *Int. J. Numer. Methods Eng.*, page in press, 2013.
- [Mue2016] R. Müller. A Benchmark problem for Phase-Field Models of Fracture. *Presentation at the annual meeting of SPP 1748: Reliable Simulation Techniques in Solid Mechanics. Development of Non-standard Discretisation Methods, Mechanical and Mathematical Analysis*, Pavia, 2016.
- [Xu94] X.-P. Xu and A. Needleman. Numerical simulations of fast crack growth in brittle solids. *Journal of the Mechanics and Physics of Solids*, 42(9):1397–1434, 1994.